1972

Simulation and performance analysis of a shipboard gas turbine emergency generator set.

Grossweiler, Philip J.

Massachusetts Institute of Technology

SIMULATION AND PERFORMANCE ANALYSIS OF A SHIPBOARD GAS TURBINE EMERGENCY GENERATOR SET

Philip J. Grossweiler

SIMULATION AND PERFORMANCE ANALYSIS OF A SHIPBOARD GAS TURBINE EMERGENCY GENERATOR SET

by

PHILIP J. GROSSWEILER III

B.S., United States Coast Guard Academy

(1966)

SUBMITTED IN PARTIAL FULFILLMENT OF THE

REQUIREMENTS FOR THE DEGREES OF

MASTER OF SCIENCE IN MECHANICAL ENGINEERING

and

MASTER OF SCIENCE IN NAVAL ARCHITECTURE AND MARINE ENGINEERING

at the

MASSACHUSETTS INSTITUTE OF TECHNOLOGY

May, 1972

SIMULATION AND PERFORMANCE ANALYSIS OF A SHIPBOARD GAS TURBINE EMERGENCY GENERATOR SET

by PHILIP J. GROSSWEILER III

Submitted to the Departments of Ocean Engineering and Mechanical Engineering on May 12, 1972, in partial fulfillment of the requirements for the degrees of Master of Science in Naval Architecture and Marine Engineering and Master of Science in Mechanical Engineering.

ABSTRACT

The objective of this study is to model and simulate using an Analog computer the performance of a relatively complex engineering system. The results of the simulation are validated by a comparison of the simulation with the measured performance of the prototype system.

The prototype system consists of a single shaft gas turbine engine driving a three-phase alternator. The alternator load is a variable speed three phase wound rotor induction motor which drives a ship bow thruster propeller. In order to provide sufficient data to validate the simulation, the alternator speed, current and terminal voltage, KW load, and induction motor speed are recorded continuously as the motor is switched through five speeds. The recorded transients in these variables are then used to validate the model and simulation.

The system is segregated into five sections and analytical models are determined for each component. The gas turbine is modeled using a transfer function derived from the engine performance curves. The speed governing system is modeled using transfer functions for the governor components as supplied by Woodward Governor Company. The alternator model is a result of the work of Professor Paynter and is taken from notes from his subject "Dynamics and Control of Rotating Machine Systems." The induction motor model is derived from a simplified equivalent circuit. The propeller is modeled as a torque proportional to the square of the speed. The simulation is simplified considerably by using a single-phase model to represent the electrical machinery.

The correlation between the simulation and the prototype performance is excellent. The models used are relatively simple and yet can provide close estimates of the system performance and can demonstrate how performance varies as the system parameters are changed.

Thesis Supervisor: Henry M. Paynter
Title: Professor of Mechanical Engineering

Thesis Reader: Warren C. Dietz
Title: Associate Professor of Marine Engineering

ACKNOWLEDGEMENTS

I would like to first thank my wife Diana for the patience she has shown during the last two years of school work, and especially during the last term.

During this study valuable assistance has been received from many individuals and in various ways. The most important has been the advice and guidance received from Professor Paynter, both during this study and in previous course work.

I am particularly grateful to Mr. Henry Egan of the Boston Naval Shipyard for providing me with the equipment required for monitoring the performance of the prototype system.

The cooperation of the United States Coast Guard First District Naval Engineering Branch and the engineers of the USCGC BOUTWELL and the USCGC CHASE was indispensible in making the required recordings of the system operation. In particular, the willingness of Chief Electrician Duke to allow an outsider to connect wires and recorders to various sections of the BOUTWELL'S electrical equipment was most encouraging. Without his willing help, it would have been most difficult to obtain system data.

Also, I would like to thank Richard S. Sidell for his assistance over the past four terms with the EAI-680 Analog computer.

Finally, I would like to thank Mrs. Jack "Sam" Price for her excellent and efficient work in typing this paper.

TABLE OF CONTENTS

LIST OF ILLUSTRATIONS AND TABLES

LIST OF SYMBOLS

ALT	Alternator
α	Governor constant
α_1	Fuel control actuator buffer spring stiffness
α_2	Fuel control actuator constant
α_3	Fuel control actuator needle valve setting
β	Propeller water velocity angle
C_τ	Propeller torque coefficient
CT	Current transformer
D	Propeller diameter
E, e	Voltage
E_1	Governor error signal
E_3	Output of governor amplifier section
FCA	Fuel control actuator
FCV	Fuel control valve
GCB	Governor control box
γ	Governor stabilizing section damping ratio
I_a	Alternator line current
I_f	Alternator field current
I_{eq}	Inertia of all components driven by gas turbine
I_m	Inertia of motor
I_p	Inertia of propeller
IM	Induction motor
K	Gain of governor amplifier section
K_f	Fuel control actuator constant

K_τ	Engine torque constant
L_a	Alternator inductance
L_m	Motor inductance
N	Speed in RPM
ΔN	Deviation of alternator speed from base speed
N_{ref}	Base speed of alternator and motor
$\dot{m}$	Air flow rate
$\dot{m}_{fb}$	Fuel flow into engine manifold
W_f'	Fuel flow into fuel control valve
W_f	Fuel flow into engine manifold
P_1	Ambient pressure
P_4	Engine exhaust pressure
PT	Potential transformer
R_2	Bearing resistance of engine and alternator
R_3	Bearing resistance of induction motor and propeller
R_a	Motor rotor resistance
R_a'	Added rotor resistance
Ψ_f	Dynamic operator representing fuel control valve action
ρ	Water density
s	Laplacian operator
Θ	Angle of fuel control actuator shaft
$\Theta_{max} - \Theta_{min}$	Maximum travel of fuel control actuator shaft
T_m	Engine mechanical time constant
τ	Torque
$\bar{\tau}$	Normalized torque (τ/τ_{ref})

τ_a	Alternator torque
τ_e	Engine torque
τ_m	Motor torque
T_1	Engine inlet temperature
T_4	Engine exhaust temperature
TF_1	Bond Graph symbol for engine speed reducer
TF_2	Bond Graph symbol for motor speed reducer
V_q	Axial water velocity through propeller
V_w	Tangential velocity of propeller blade at maximum diameter
ω	Speed in radians per second
ω_s	Motor synchronous speed
X	Electrical reactance
X_{eq}	Equivalent reactance of motor
X_{sa}	Synchronous reactance of alternator

1. INTRODUCTION

Simulation has become one of the most important tools available to engineers in the study and design of complex physical systems. The ability to predict a system's response to various inputs is useful in many ways. Actions which can have disastrous effects on a system can be avoided if accurate predictions of the system response are available. Simulation can also aid in the realization of high levels of system performance by aiding in control system design. Studies of the effects of varying system parameters can be performed with a simulation so that an optimum or near optimum prototype can be built without a costly trial and error process.

The first stage in simulating a complex physical system is to identify the individual components. An attempt is then made to formulate a model for each component of the system so that the interconnected models will predict the performance of the system within a specified level of accuracy. Simulation is in effect a four-stage process. In the first stage the system is reduced to individual components and "black boxes" are used to represent these components. In the second stage, the components are interconnected so as to reflect the structure of the prototype system. The third stage usually requires the use of a computing machine to determine the time history of the variables as the components interact with each other.

This simulation procedure can be carried out almost completely using the concept of Bond Graphs (1), (2). Although bond graph techniques can be used to develop a set of state equations representing the entire

system, for this simulation bond graphs will be used primarily to display the structure of the system. The Bond Graph method enables one to visualize a system as a set of multi-port devices connected by power bonds. As a result of this partitioning of the system the energetic interactions across the boundaries are clearly shown. For the case of the prototype system under study the basic bond graph representing the main power flow is as follows:

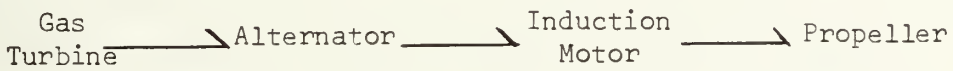

Each component is a multiport which interacts with the rest of the system through the power bonds as shown. Associated with each bond are the power variables (T, ω or e, i) which determine the power flow between the multiports.

The models required for the multiports shown above can be determined in various ways. However, regardless of how the models are determined, they should satisfy the following conditions:

1) The time history of the power variables at each port when connected to the system should in the simulation match that of the corresponding prototype parts over the ranges of variables and frequencies being considered.

2) Each model should be as simple as possible consistent with the accuracy required for the simulation. Unnecessary complexity will increase the cost of simulation and will tend to obscure the more important points. More important however is the need to adapt the simulation to available computer facilities. Frequently, as in this case, the

simulation must be simplified because of limitations of the available computing equipment.

There is no unique method of modeling system components. However, any method can be classified as being either analytical or empirical. Analytic methods rely on use of the basic engineering disciplines and in effect derive a model from first principles. Although in principle analytic methods can be used to model any device, these methods become extremely difficult to use for very complex components. Empirical methods are in effect a transfer function approach to modeling. Given a component and information about its performance under specified conditions, it is usually possible to infer a relationship between the input and output variables. For multiple input-multiple output systems this technique may become difficult to use. Also, this method gives no information about the internal operation of the component. However, for studies where only interactions with the rest of a system are considered this method is perfectly adequate.

In this study the models are determined using both methods. The alternator model is based on an analytic derivation whereas the model for the gas turbine is derived from performance curves. The models used for this simulation are discussed in detail in the following sections.

The question most frequently asked during this study was "Why simulate a system which has already been built?" The final stage in any simulation is validation of the results. Although in most cases the simulation must be validated without prior knowledge of the prototype, models which have been proven with one prototype can be used with great confidence for a large family of similar systems. In effect, the best

documentation of a system model is by comparison with observed performance of a prototype. A large part of this study deals with collecting sufficient operating data from the prototype system in order to validate the models used.

The prototype was selected because it provided the opportunity to model an interconnected system which included mechanical and electrical machinery with feed-back control on the energy source. Equally important was the ability to instrument the system in order to record sufficient operating data to validate the model. The prototype selected was the gas turbine emergency generator set and bow propulsion system on the USCGC BOUTWELL which is located in Boston, Massachusetts. The purpose of this study is to simulate the effects of the transients in the system caused when the bow thruster motor is started.

2. DESCRIPTION OF PROTOTYPE SYSTEM

The prototype system is shown in detail in the bond graph shown in Figure 1. The prototype system is defined from an arbitrary choice of equipment installed on the ship. The emergency generator can be used to supply electrical power to any load on the ship as shown in the sketch below. The bow thruster is a trainable propeller which is used to provide a directional thrust at the bow when docking the ship. The unit is retracted into the ship when not in use. The electrical system can be interconnected so that the bow thruster is the only load on the emergency generator. The prime mover is a single shaft Solar Saturn Gas Turbine. For standard atmospheric conditions the engine is rated at 1200 HP at 22,300 RPM. The output is reduced through a two stage planetary gear box to 1200 RPM. An engine cutaway view, arrangement of reducing gear and engine performance curves are given in Figures 2, 3, and 4.

The engine speed is controlled by a Woodward EG series governor. The governor system is shown in the schematic on page 20. The two main components are the EGA Control Box and the EGB-2C Actuator. The governor can control the engine in either isochronous or droop mode. The actuator can also control the speed using the conventional mechanical flyweight assembly. For this study the system will be controlled electrically and in the isochronous mode. The operation can best be described by the transfer functions for the components. The transfer functions supplied by Woodward Governor Company are of the following form:

$$E_1 = \frac{-1.5\ \Delta N}{N_R E} + \frac{0.00405\ S}{s/10 + 1} \quad \frac{\tau_e}{\tau_{REF}} \qquad \text{(error signal)}$$

$$\frac{E_3}{E_1} = \frac{K\ (s + \alpha)}{s^2 + \gamma s + \sigma} \qquad \text{(amplifier section)}$$

$$\frac{\Theta}{E_3} = \frac{33.3\ \alpha_2 (s + \alpha_3)}{s(s + \alpha_1)} \qquad \text{(EGB-2C Actuator)}$$

These signals are shown in the governor schematic, Figure 5.

The error signal is a combination of a voltage proportional to the error in speed and a voltage output from the load sensing network which provides lead compensation. The governor response can vary over a wide range depending on the values of the following parameters:

(1) Feedforward gain of the load sensing network (0.00405)

(2) Gain of the amplifier section (K)

(3) Damping ratio of the stabilizer section (γ)

(4) Buffer spring stiffness (α_1)

(5) Needle valve setting (α_3)

The alternator is a General Electric machine with the following characteristics:

Rated KVA	625	Speed	1200 RPM
Rated KW	500	Winding	3 Phase
Rated P.F.	0.8	Connection	Y
Rated Volts	450	Frequency	60 Hz
Rated Amps	801	Poles	6

Voltage regulation is provided by a static excitation system.

The alternator is connected to the ship's electrical system in the following way.

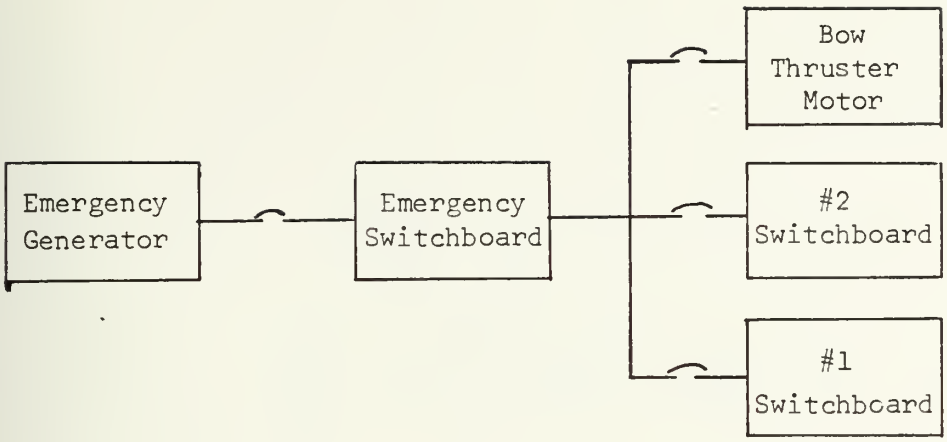

For this study the system is set up so that the emergency generator is supplying only the Bow Thruster load.

The Bow Thruster Unit is shown in Figures 6 and 7. It is manufactured by Schottel of America, Inc. The driving motor is a General Electric three-phase wound rotor induction motor with the following ratings:

Rated Volts	440	Rated Amps	440
Speed	1180 RPM	Torque	1550 lb-ft
HP	350	Frequency	60 Hz

The motor performance curves are shown in Figure 11. The motor is started with full line voltage applied and additional resistance in the rotor circuit. Five propeller speeds are provided by shunting the external resistors in four steps. The shunting of these resistors is controlled by time delay relays. The motor is connected to the propeller through a vertical shaft and bevel gears.

The propeller is enclosed in a nozzle as shown on page 22. The diameter is four feet, pitch 28.819 inches and the reduction ratio from the motor speed 2.079:1.

Figure 1.

PROTOTYPE SYSTEM BOND GRAPH

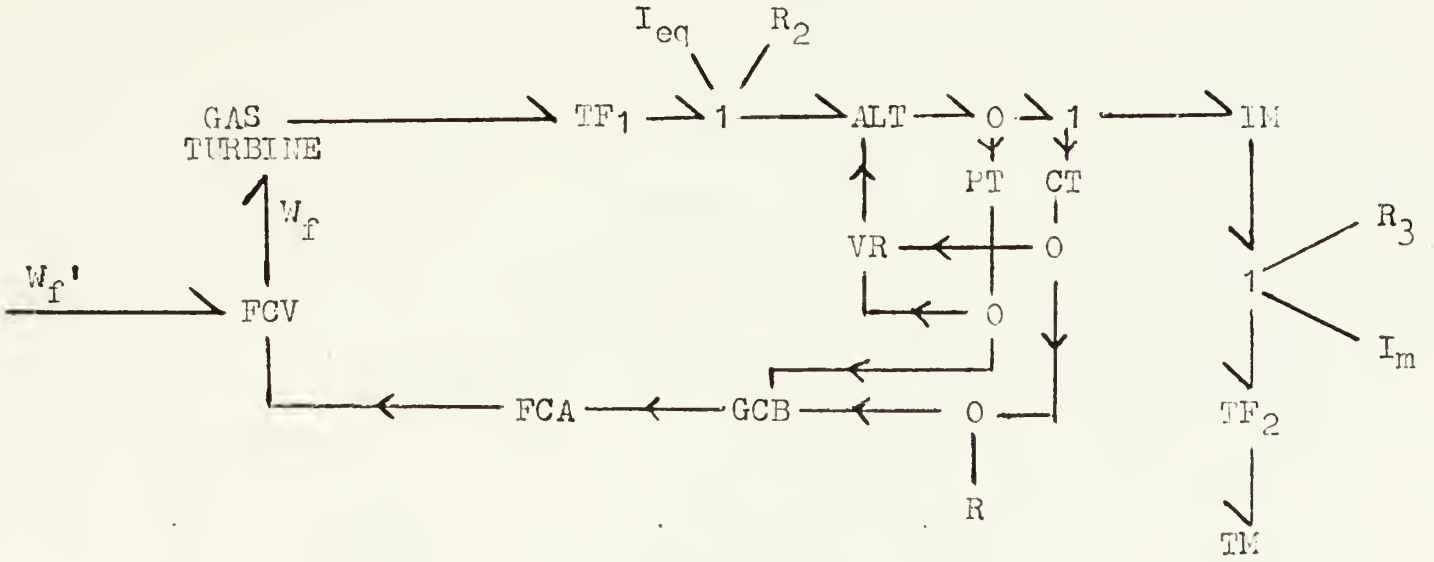

Figure 2.

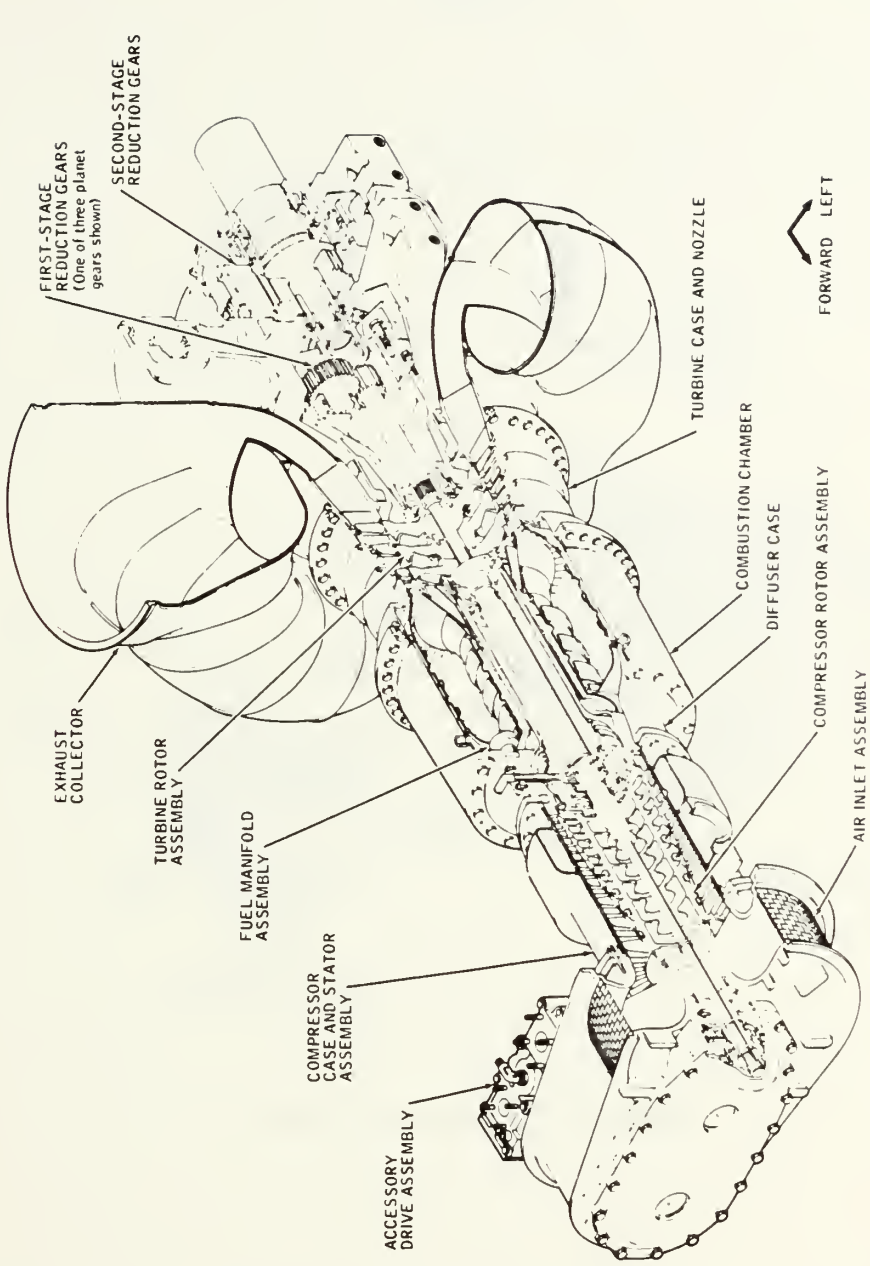

Figure 1-2. Cutaway View Typical Saturn Gas Turbine Engine

Drawing Courtesy of SOLAR Inc.

Figure 3.

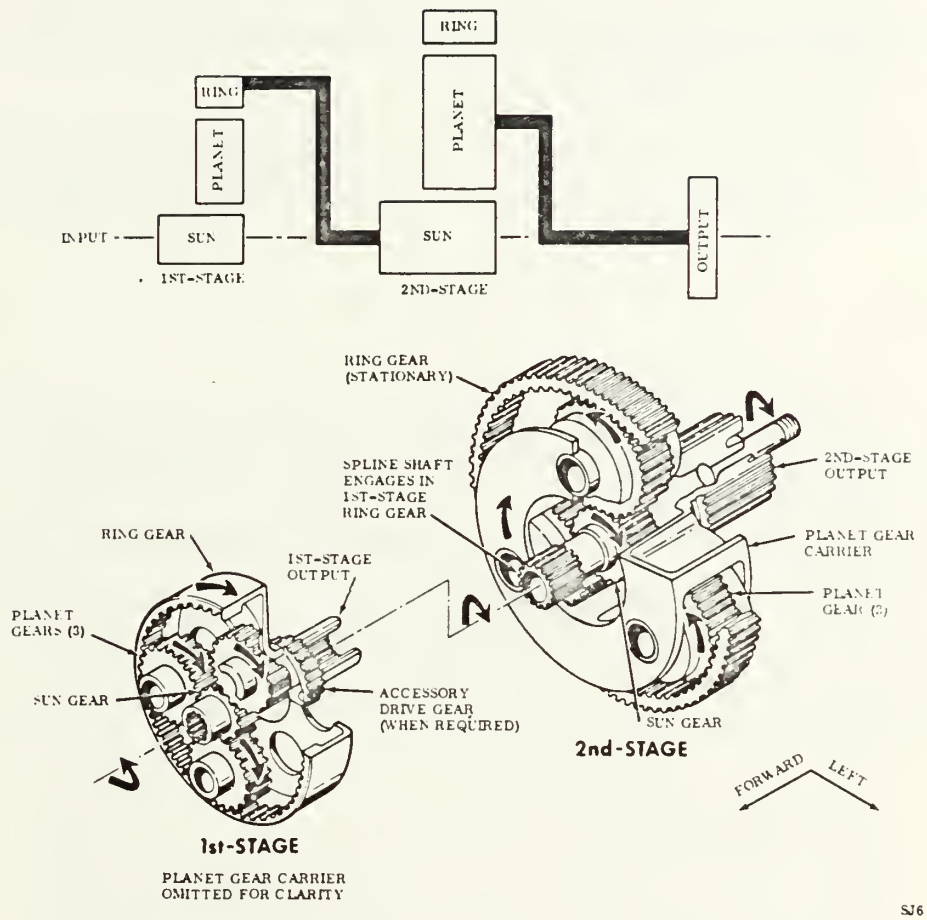

Drawing Courtesy of SOLAR INC.

Figure 4.

- TYPICAL PERFORMANCE SATURN GAS TURBINE ENGINE 500 KW GENERATOR
- ZERO INLET AND EXHAUST DUCT PRESSURE LOSSES AT 100 PERCENT RATED ENGINE SPEED
- SEA LEVEL
- THE TURBINE GENERATOR SET IS RATED AT 500 KW, 0.8 PF. MAXIMUM CONTINUOUS OPERATION WITH OVERLOAD CAPABILITY OF 10 PERCENT FOR 2 HOURS IN ANY 24 HOUR PERIOD.

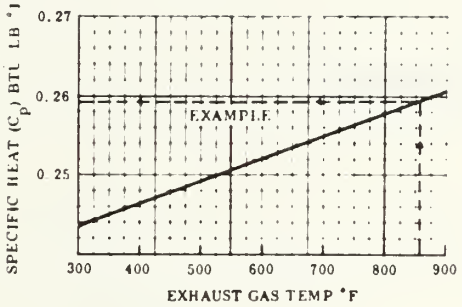

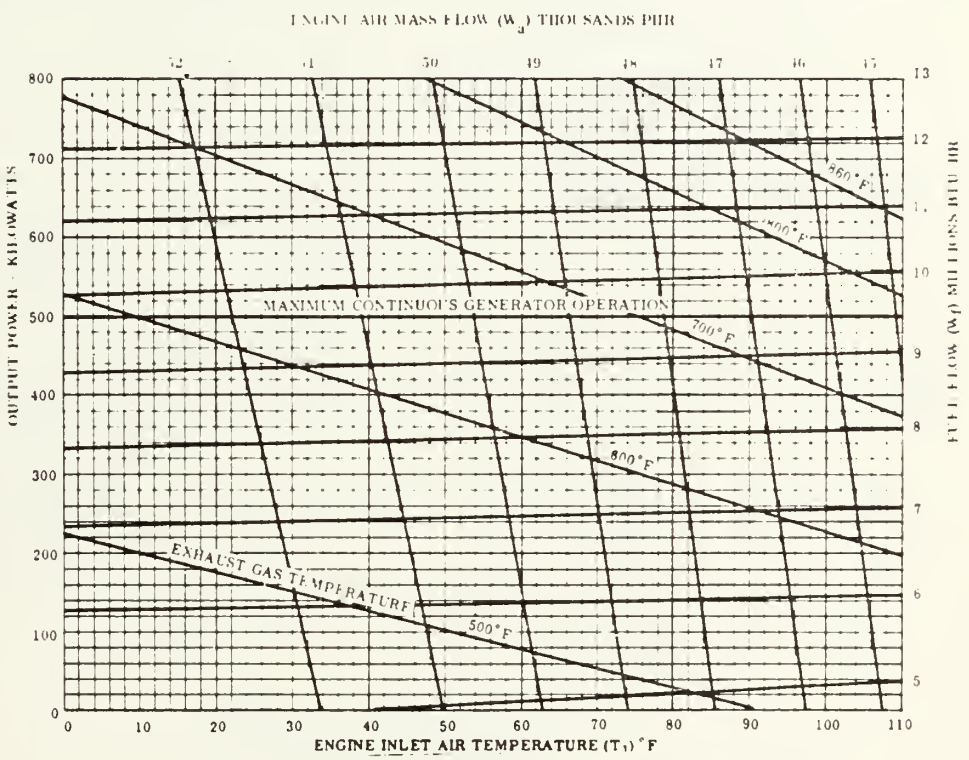

Output Power (KW) vs Engine Inlet Air Temperature

Drawing Courtesy of SOLAR INC.

Figure 5.

Governing System Schematic

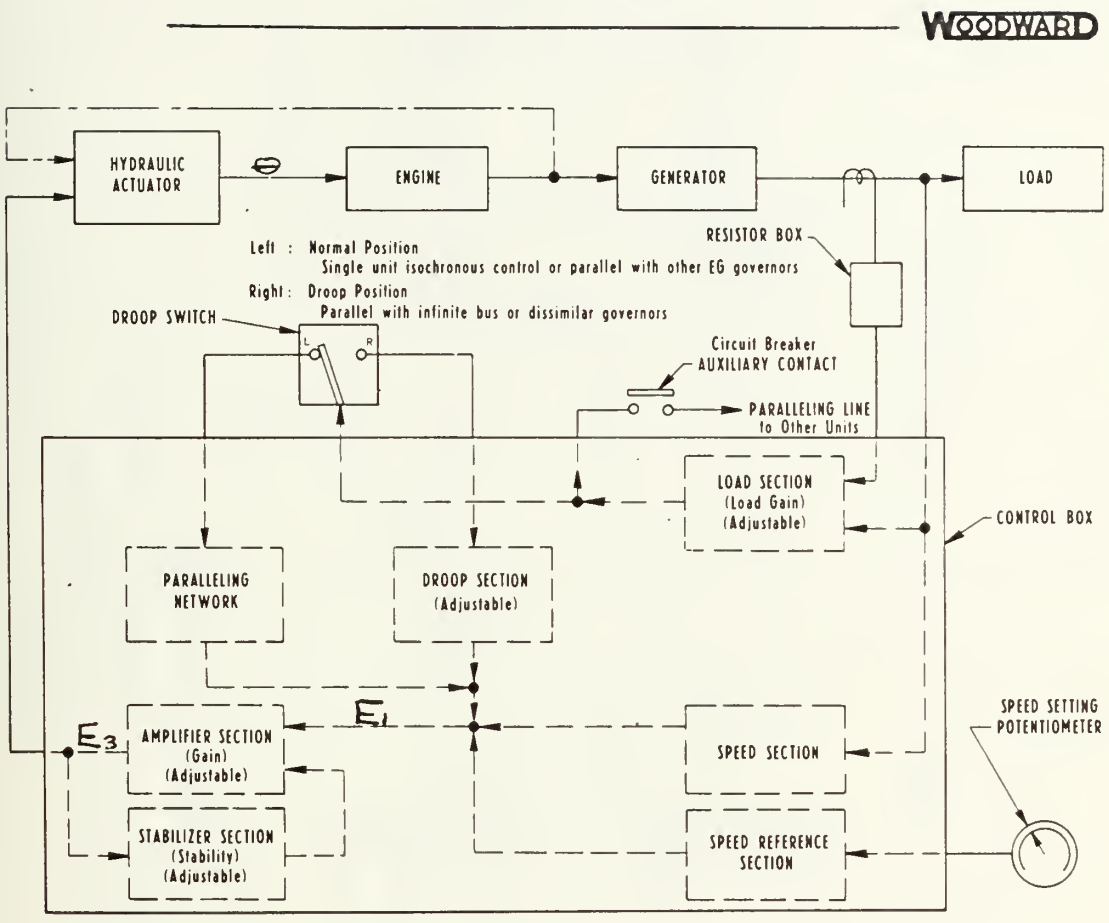

Drawing Courtesy of
WOODWARD GOVERNOR COMPANY
(Bulletin 37706B)

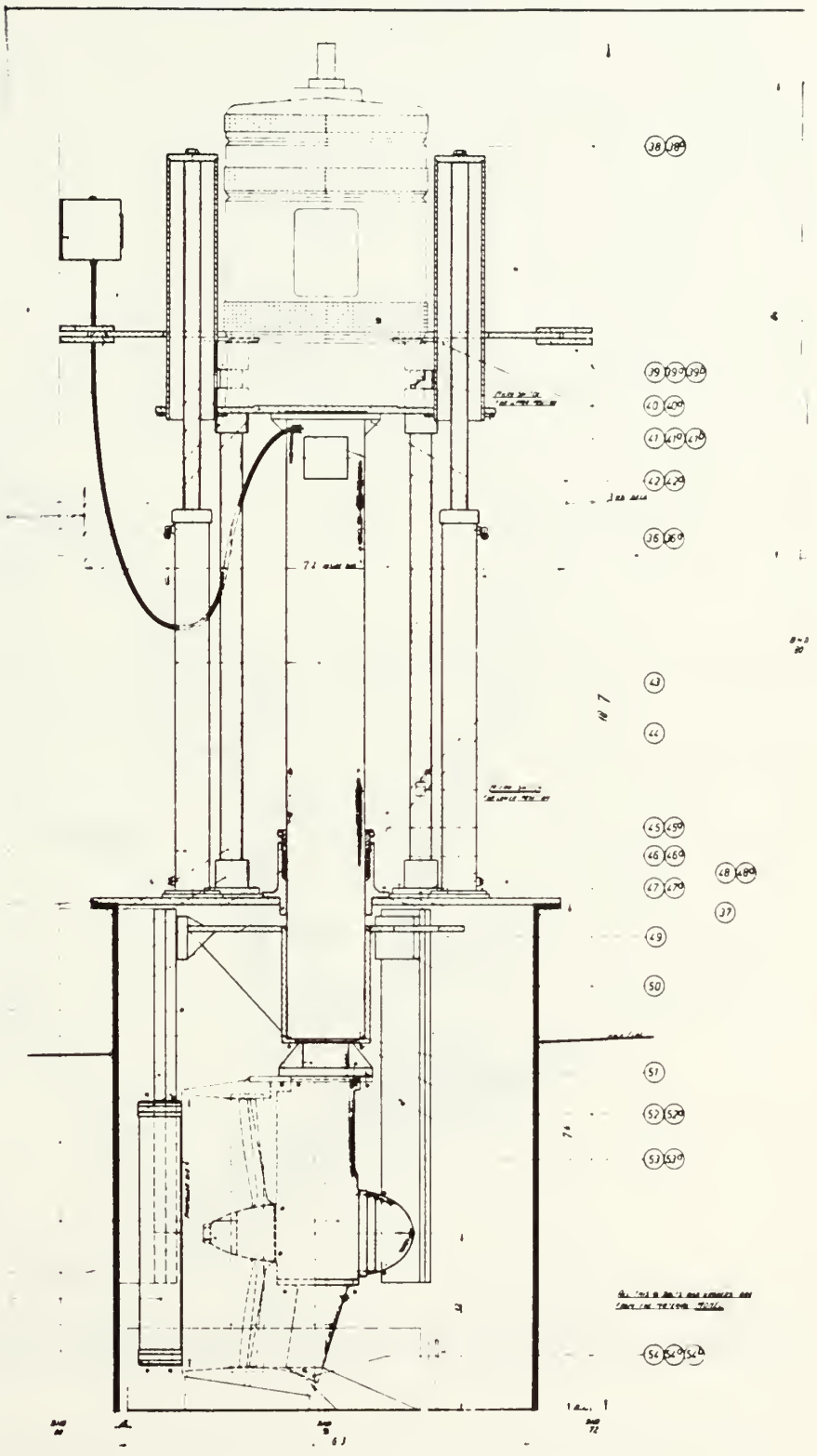

Figure 6.

Schottel Bow Thruster Arrangement

Drawing Courtesy of SCHOTTEL of AMERICA INC.

Drawing Number 865-3

Figure 7.

Bow Propeller With Nozzle

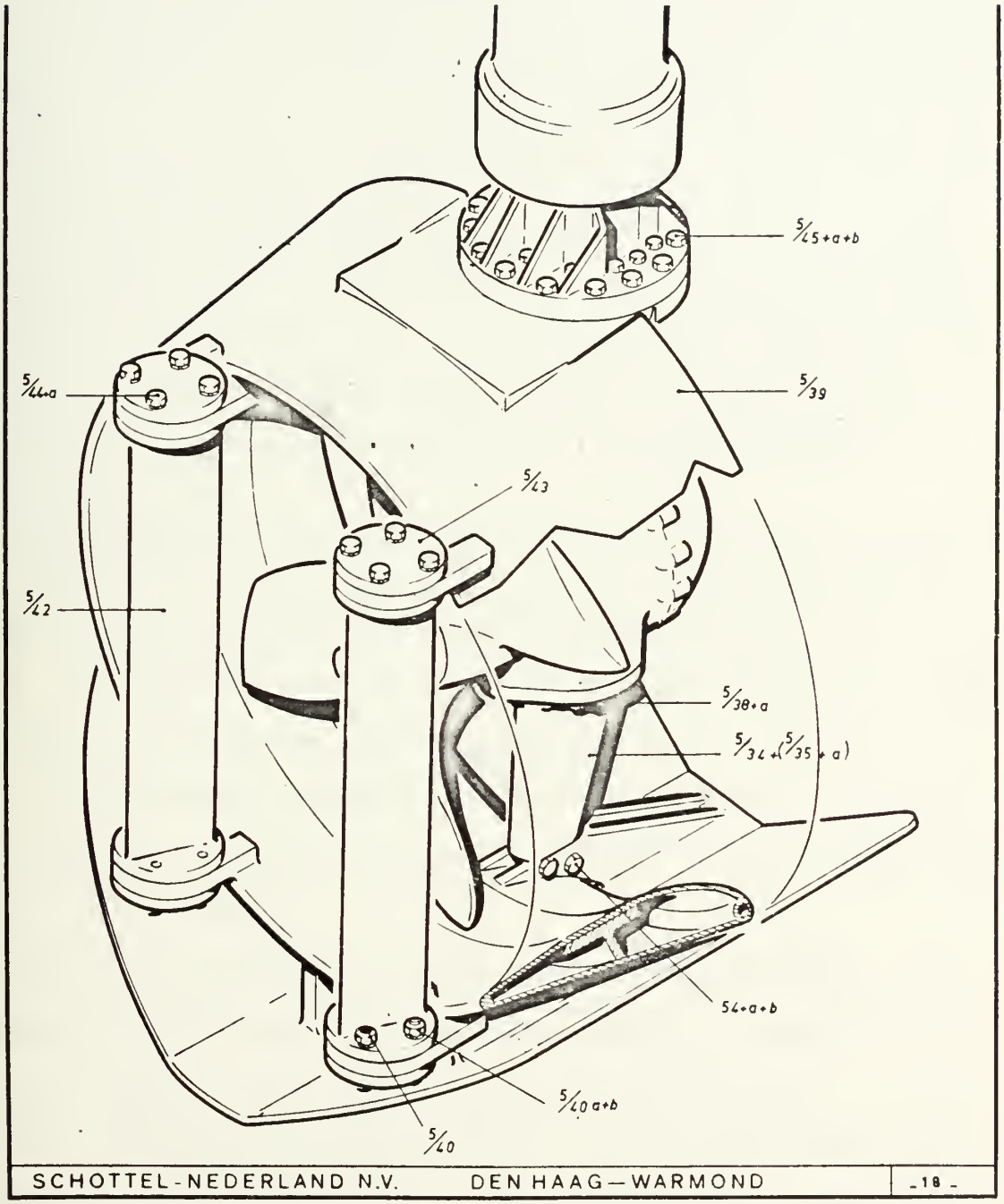

3. INSTRUMENTATION AND RECORDING

Verification of the system model and simulation by comparison with the prototype performance requires records of the system variables during operation. The optimum choice for recorded variables are the state variables of the system model. In this case the choice of observed variables was limited to measurements which could be made without major modifications to the prototype and which did not require excessive time or cost. As a result, most of the observed variables were chosen because the prototype was instrumented to monitor these variables. However, these constraints did not prevent obtaining a set of observables sufficient for model verification.

The complete instrumentation setup is shown in the bond graph in Figure 8. The main power flow through the system is shown with heavy lines. The boxed items show all sensors, signal conditioners and recorders which were added to the prototype instrumentation. Each box is labeled with the variable recorded. All bonds to the boxes are active, i. e., zero power flow into the recorders is assumed. Details of each measurement is given below.

Results were recorded on a Clevite Mark 220 Brush Recorder. This instrument is very versatile and provided satisfactory records of all variables measured. Input signals ranged from five millivolts to fifty volts and in frequency from D.C. to 60 Hz. For full scale deflections the frequency response is flat up to 40 Hz. The frequency response can be increased to 100 Hz if the meter movement is limited to twenty percent of the full scale.

ALTERNATOR LOAD The EGA Control Box Load Section senses the

alternator terminal voltage and current through potential and current transformers. A correction is made for power factor so that the output of the load section is a signal with a D.C. level proportional to the KW load. At full load the D.C. level is approximately nine volts. However, this value will vary depending on the values of the resistors used with the current transformers, the levels of voltages and currents delivered by the instrument transformers and the gain of the load sensing section.

The load signal contains harmonics of the line frequency in addition to the D.C. level. Since the amplitude of these harmonics was approximately twenty percent of the D.C. level an RC low pass filter with a time constant of 0.068 seconds was used to filter the harmonics.

FIELD CURRENT The full load field current is approximately seventy amps at seventy volts. A shunt resistor was inserted in the field circuit at the brush rigging. The shunt resistor voltage drop is fifty millivolts at seventy-five amps.

ALTERNATOR SPEED The installed tachometers and frequency meter are used primarily for steady state observations. Large errors in measuring transients can be expected when the time interval of the transient approaches the time constants of the meter movements. As a result, the meters cannot be used to accurately record transients resulting from step changes in load.

The speed measurement was made using a Clevite Corporation Frequency Converter. The converter is calibrated to give a D.C. signal proportional to the change in frequency. A deviation of ± 5 Hz from the base frequency gives a ± 2.5 volt output. The rise time of the output signal is 0.060

seconds. This response together with the response of the recorder gives an accurate measure of the speed transient.

The signal input to the converter is at 110 volts in the range 55-65 Hz. The prototype system was set up with the alternator supplying the emergency switchboard so that the bow thruster was the only load. In order to provide a 110-volt signal at the alternator frequency for input to the converter, the 110-volt lighting circuit at the emergency generator was supplied from the emergency board. This total lighting load is less than five KW so that the effect on the alternator is negligible. The alternator load is assumed to be from the bow thruster motor only.

TERMINAL VOLTAGE The terminal voltage was recorded using a Clevite Corporation Volts Converter. The recorder delivers a D.C. voltage proportional to the peak A.C. voltage. The converter was driven by the 220 volt output of the load sensing network potential transformer.

ARMATURE CURRENT The armature current was recorded from the voltage across the input resistors to the load sensing network. The current to these resistors is supplied by the current transformers connected across the main line. Since this signal was at the 60 Hz line frequency the maximum amplitude of the recorded signal was limited to approximately twenty percent of the chart deflection in order to have satisfactory frequency response.

BOW THRUSTER SPEED The induction motor drives an A.C. tachometer generator. The tachometer output was recorded directly on the Brush Recorder. Speed can be determined either from the instantaneous frequency or voltage amplitude. For 1200 motor RPM the tachometer frequency is

40 Hz. The tachometer signal was recorded full scale on the chart since the recorder frequency response is flat to 40 Hz.

Figure 8.

INSTRUMENTATION BOND GRAPH

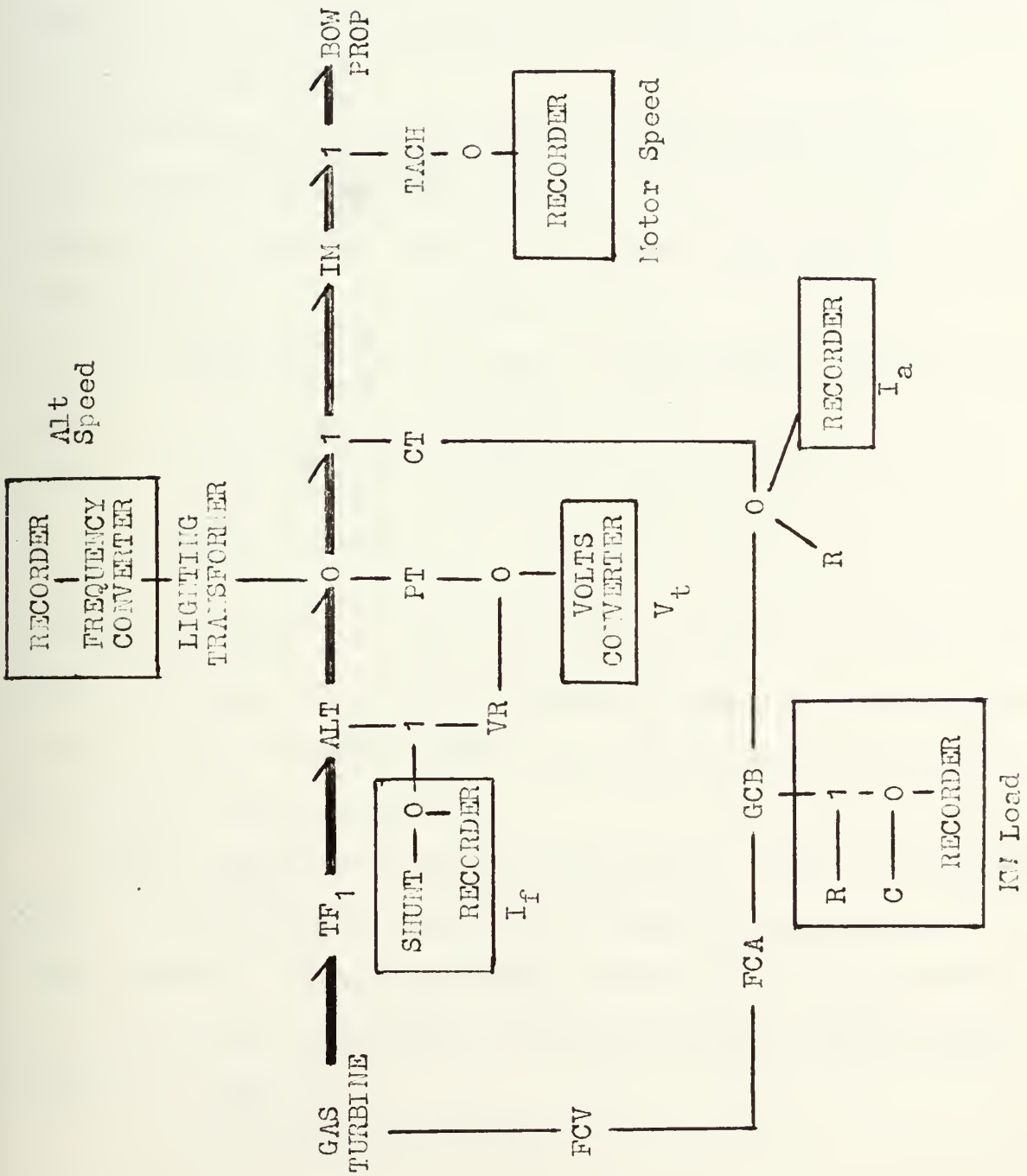

4.1 GAS TURBINE MODEL The derivation and final structure of the gas turbine model depends on the type of study involved. In one type of study, knowledge of internal behavior in response to changes in environment and load is required. In other studies, only knowledge of the time history of the input/output variables is required. Obviously for the latter case the model can be simpler and will most likely be in the form of a transfer function.

In reference (10) a model is derived from basic principles for a single shaft gas turbine where it is shown that the gas turbine can be represented by a multiple input-multiple output transfer function of the following form.

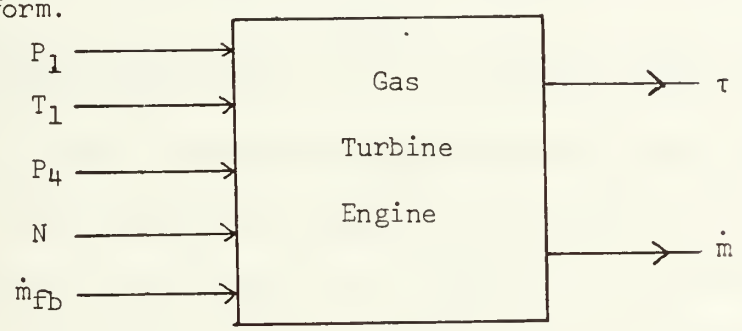

The matrix representing the input and output vectors is a relatively complicated non-linear function of the internal variables and engine characteristics. For this case the model can be simplified considerably and will be used in a linearized form.

The most valuable information provided by this formulation is an indication of the functional relationships which exist between the input and output variables. Since the mass flow rate ($\dot{m}$) is not being considered, only the functional relationship for torque is needed. From the transfer function it is seen that

$$\tau = \Phi(P_1, T_1, P_4, N, \dot{m}_{fb})$$

For this study, the ambient conditions P_1 and T_1 can be assumed constant. For a constant mass flow rate, fixed geometry and constant ambient conditions the exit pressure P_4 is also relatively constant. Since the mass flow rate is primarily a function of the speed, which is relatively constant, the only input variable which changes significantly is the fuel flow rate $\dot{m}_{fb}$. As a result the functional relationship can be reduced to:

$$\tau = \Phi'(\dot{m}_{fb})$$

This functional relationship can also be derived by considering a control surface around the engine.

For this case where the engine can be considered small with respect to its ability to store energy as a result of either mass or thermal capacity, the changes in stored energy can be neglected. From observations on the prototype, it is known that the temperature of the exhaust gas is relatively constant throughout the operating range. With a constant air flow rate and exit velocity the enthalpy of the entering and leaving gases is relatively constant. As a result, the primary energy quantities entering and leaving the control surface are in the fuel flow and shaft work. With all of the assumptions above it is seen that output power is proportional to input fuel. Since speed is relatively constant it follows that

$$\tau = \Phi'(\dot{m}_{fb}) = K_\tau \dot{m}_{fb}$$

This relationship is verified by the engine performance curves given in Figure 4. Since the output KW is proportional to torque at constant

speed, the torque is proportional to fuel flow rate for constant T_1.

In a simulation, it is necessary to consider the effects of the engine dead time or transport delay. This delay is defined as the time interval between a change in fuel flow rate and the change in torque output. From the control surface above, it is seen that this delay depends on the ability of the engine to store energy and the speed at which changes in internal temperature resulting from fuel rate changes can propogate through the engine. As stated above, the storage effects can be neglected. An estimate of the delay due to propagation time can be made by considering the transit time for sound waves through the engine. This is the speed at which the temperature changes resulting from fuel rate changes propogate. For the Saturn engine, the transit or dead time is on the order of 0.005 seconds. The torque relationship is then modified as follows:

$$\tau = K_\tau' e^{-Ts} \dot{m}_{fb} \cong \frac{K_\tau' \dot{m}_{fb}}{1 + Ts}$$

The delay is approximated by a first order lag for the purposes of analog computation.

All that is necessary to develop the turbine model is to determine the torque coefficient from the performance curve. This coefficient is a function of ambient temperature with K_τ decreasing with increasing ambient temperature. It will be shown below that when the system block diagram is non-dimensionalized for the analog computation, the torque constant can be lumped with the overall loop gain.

4.2 GOVERNOR SECTION The governor schematic is shown in Figure 5. The engine block diagram can be formulated directly from the schematic using the governor transfer functions supplied by Woodward Governor Company.

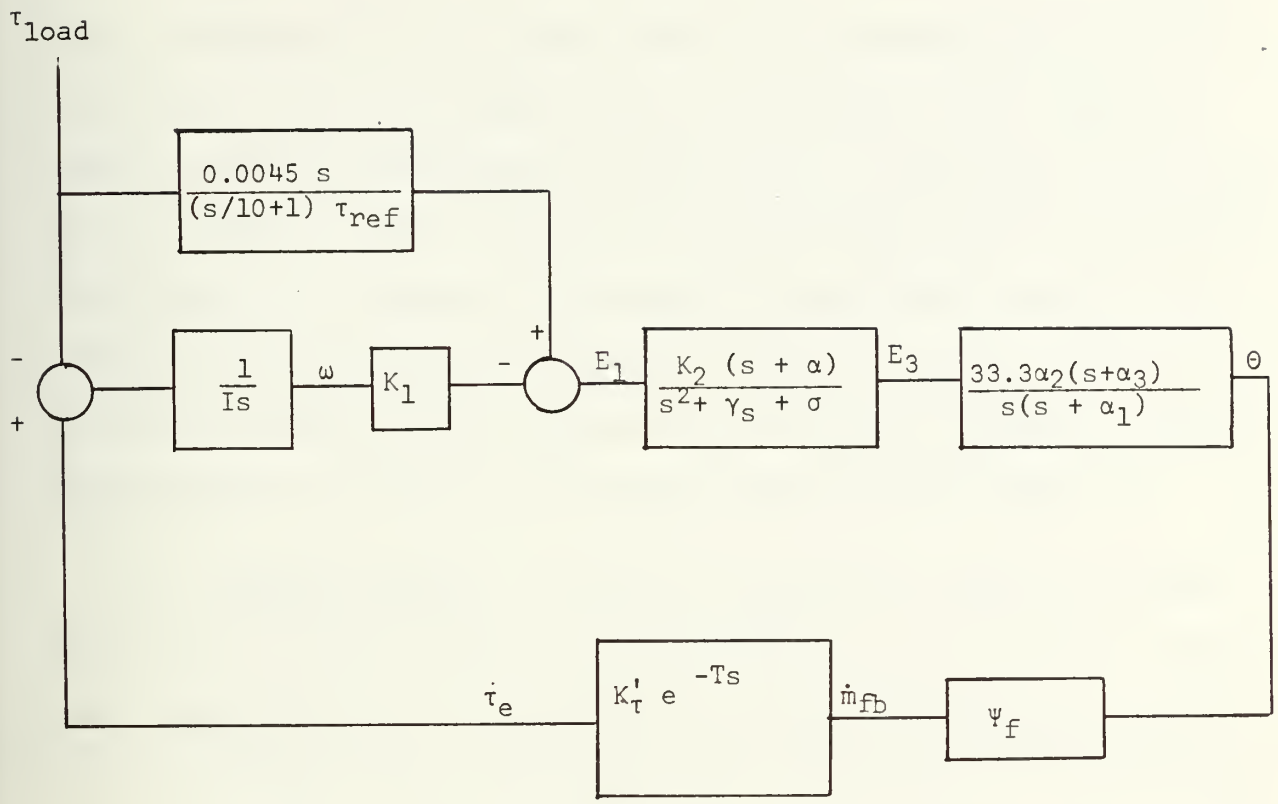

Figure 12.

From the diagram it is seen that if the delay is neglected

$$\tau_e = K_\tau' \dot{m}_{fb} = K_\tau' \Psi_f \, \Theta = K_\tau' K_f \, \Theta$$

where it is assumed that the fuel flow is proportional to the angle of the fuel control valve. Although in most cases this relationship is approximately linear, slight non-linearities will not affect the overall system performance. Although the fuel control valve is actually a dynamic operator, in this case the valve will be considered to be a static operator. For low frequency changes in fuel angle this is a good approximation. With $K_\tau = K_\tau' K_f$; $\tau = K_\tau \Theta$ Taking $\tau = \tau_{REF}$ when $\Theta = (\Theta_{max} - \Theta_{min})$, where $(\Theta_{max} - \Theta_{min})$ is the maximum travel of the fuel control actuator, the torque constant K_τ is

$$K_\tau = \frac{\tau_{REF}}{\Theta_{max} - \Theta_{min}} \quad .$$

In reference (10) it is shown that if the loop gain K_2 is not excessive the gain and phase margins at the crossover point of the open loop transfer function (approximately 6 rad/sec) will be adequate and the action of the stabilizer section of the control box $\left(\frac{1}{s + \gamma_s + \sigma}\right)$ can be neglected. This simplification neglects the response of the governor system to frequencies above approximately 50 rad/sec. With the stabilizer section neglected and using the nominal values for the governor settings, the system block diagram is as shown in the section on Analog Scaling page 58.

4.3 ALTERNATOR MODEL The study of alternators typically involves deriving an equivalent circuit and phasor diagram of the electrical variables. However, the phasor diagram does not explicitly show the mechanical-electrical energy conversion process which is a major part of the prototype system's power interactions. The model used for the simulation must include the torque-current and speed-voltage relationships involved in the energy conversion process. Such a model can be derived from a study of the energy interactions of idealized magnetic circuits. The model proposed by Paynter, reference (10),was formulated this way and as a result shows the structure of alternator as a gyrator-type converter as well as the behavior of the electrical variables.

The major assumptions required to simplify the analytical derivation of the alternator model are that the magnetic circuits are not saturated and that all fluxes are linear functions of the currents. The linearization reduces the problem to a study of linear-coupled circuits and allows superposition of the magnetic fields. It is also assumed that the air gap is uniform. However, in a study of terminal voltage, current, torque,

and speed relations under load conditions, salient pole effects are relatively minor and can be neglected. One of the main effects of saliency is to produce a reluctance torque, and, except at no load, this torque is negligible compared to the total torque. The resulting model can then be used for machines which are operated under quasi-linear conditions and can be used for modeling the prototype alternator.

The basic variables and relations required for the derivation are as follows:

$\lambda \equiv$ flux linkage $= N\phi$

$N \equiv$ effective turns ratio of winding

$\phi \equiv$ equivalent flux linking all terms $= PF$

$P \equiv$ permeance

$F \equiv$ magnetomotive force $= Ni$

$W_m^* \equiv$ co-energy in magnetic field $= \int_0^F \phi(F)dF = \int_0^i \lambda(i)di$

The inherent behavior of polyphase machines is the same regardless of the number of phases. As a result the torque is determined by the current flowing in each phase and the number of phases. In the balanced polyphase machine each phase torque is a pulsating torque at twice the line frequency with a D.C. level which is exactly the total torque divided by the number of phases. When all phase torques are summed the pulsating torques cancel so that the total torque is constant in the steady state.

A reasonably accurate model of the alternator (and motor) can be made using only a single phase if the torque pulses can be neglected. Alternators with large inertias behave dynamically as low pass filters as seen from the simplified bond graph and system equations for a rotating mass.

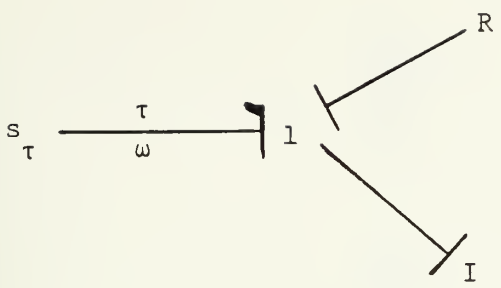

Where $\frac{\omega}{\tau} = \frac{1}{Is + R}$ Where $I = \frac{WR^2}{g}$

For the prototype system I is on the order of 2000 lb-ft^2 and 2ω the frequency of the torque pulsations is 754 radians per second. Since R is relatively small;

$$\left| \frac{\omega}{\tau} \right| \approx \frac{1}{\frac{2000}{32} \times 754} << 1$$

where ω is the fluctuation in speed caused by the pulsating torque.

The inertia of the induction motor and load is the same order of magnitude so that a single phase model can be used for both with torque pulsations being filtered by the relatively large inertias.

The alternator model used below is taken from one phase of a two-phase alternator model. Although the model is derived for a two-phase machine, one phase can be used to represent one phase of a three-phase machine since the torque pulsations are both double-frequency pulsations and are filtered by the inertias. All that is required to use this model for a three-phase machine is to properly scale the D.C. level of the torque.

The two-phase representation shown below is very similar to the Park's dqo transformation used in studying three-phase machines. In this case the variables are referred to the two-phase stator whereas in the dqo transformation the variables are viewed with respect to the rotor.

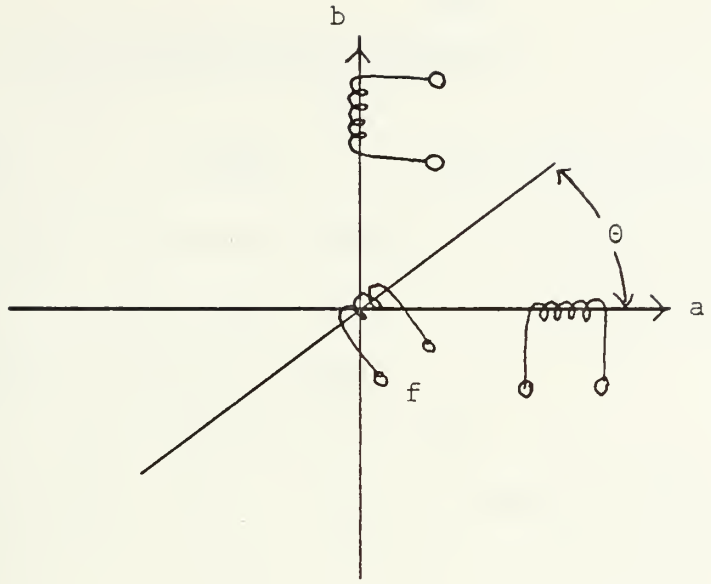

Total flux linking coil a

$$\lambda_a = N_a P[N_a i_a + N_f i_f C] \qquad (1)$$

Total flux linking coil b

$$\lambda_b = N_a P[N_a i_b + N_f i_f S] \qquad (2)$$

Total flux linking coil f

$$\lambda_f = N_f P[N_a i_a C + N_a i_b S + N_f i_f] \qquad (3)$$

Where $N_a = N_b$ $\qquad M \equiv N_a N_f P$

$C \equiv \cos\Theta$ $\qquad N \equiv N_a^2$

$S \equiv \sin\Theta$

and the permeance is independent of Θ in accordance with the assumption of a smooth air gap.

Now $W_m^* = \int[\lambda_a di_a + \lambda_b di_b + \lambda_f di_f]$

$$W_m^* = \int[PNi_a di_a + CMi_f di_a + PNi_b di_b + SMi_f di_b + CMi_a di_f + SMi_b di_f + PN_f^2 i_f di_f] = \tfrac{1}{2}PN[i_a^2 + i_b^2] + \tfrac{1}{2}PN_f^2 i_f^2 + Mi_f[Ci_a + Si_b] \qquad (4)$$

For any electro-mechanical converter

$$\frac{\partial W_m^*}{\partial \theta} = \tau \qquad \text{so that} \qquad \tau = Mi_f\,[-S\,i_a + Ci_b]$$

The exact relationship between τ, ω, e and i is found from a consideration of power balance.

Assuming a lossless system:

$P_{mech} = P_{AG}$ (developed at air gap)

$P_{elect\ output} = P_{AG} - P_{stored}$ (in magnetic field)

The alternator is in effect separated into two processes, energy conversion and energy storage. Equating power at the air gap yields the following identity:

$$\tau\omega = P_{AG}$$

Where for a two-phase machine

$$\tau\omega = e_a i_a + e_b i_b$$

$$Mi_f\omega\,[-Si_a + Ci_b] = e_a i_a + e_b i_b$$

$$\text{or } e_a = [-SMi_f]\ \omega = R_a\,\omega$$

$$e_b = [CMi_f]\ \omega = R_b\,\omega$$

Where $R_a = -SMi_f$ and $R_b = CMi_f$

in matrix notation

$$\begin{bmatrix} e_a \\ e_b \\ \tau \end{bmatrix} = \begin{bmatrix} 0 & 0 & R_a \\ 0 & 0 & R_b \\ R_a & R_b & 0 \end{bmatrix} \times \begin{bmatrix} i_a \\ i_b \\ \omega \end{bmatrix}$$

If τ is separated into its two components the gyrator-like action of the energy conversion is evident.

$$\tau_a = R_a i_a \qquad e_a = R_a\omega$$

$$\tau_b = R_b i_b \qquad e_b = R_b\omega$$

The magnetic energy can be modeled as an I field. The three currents i_a, i_b, and i_f are the sources of the stored magnetic energy. Since

$i_f \ll i_a$ and

$i_f \ll i_b$

most of the energy is stored as a result of the armature currents so that changes in armature currents will account for most of the change in stored energy. This implies a model of the form

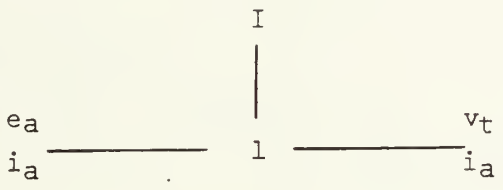

which is in fact the equivalent circuit of an alternator with negligible armature resistance.

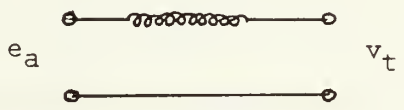

The bond graph for the complete conversion process is:

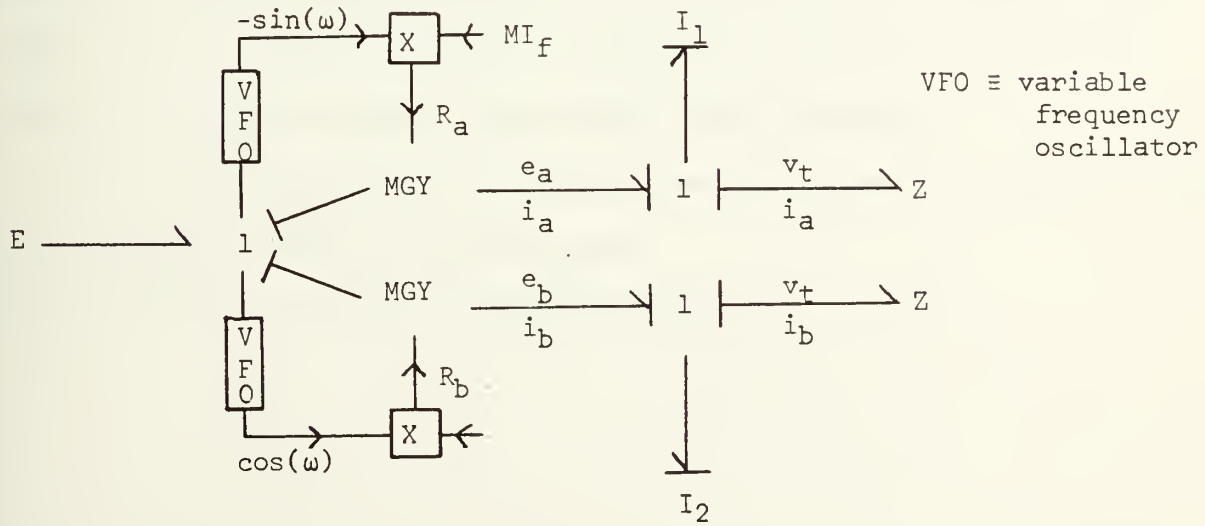

where E represents the prime mover. The causality of E is determined by the structure of the complete system. The Analog simulation of this model will represent the exact alternator behavior (within the limits of original assumptions). However, the model requires six multipliers. The need to minimize Analog hardware required for simulation makes it necessary to use the single-phase model.

For this case

$$\tau_a = R_a i_a$$

$$= -MI_f \sin(\omega t)\, i_a$$

for $i_a = I_a \sin(\omega t - \phi)$ where $\Theta \equiv \omega t$

$\phi \equiv$ phase angle between i_a and e_a

$$\tau = -MI_f I_a \sin(\omega t) \sin(\omega t - \phi)$$

$$= MI_f I_a \sin(\omega t) \sin(\omega t - \phi)$$

$$= \tfrac{1}{2} MI_f I_a [\cos\phi - \cos(2\omega t - \phi)]$$

Whereas $\tau_a + \tau_b = MI_f I_a \cos\phi$;

τ_a alone gives a D.C. value equal to ½ of the actual steady torque plus a double frequency pulsating value. As shown above the alternator rotating mass has a large amount of inertia and acts as a filter for the high frequency torque pulsations. As a result, the one phase approximation can be used without any appreciable loss in accuracy.

The total torque input to the prime mover can then be obtained merely by doubling the torque calculated above.

For the simplified model the bond graph becomes:

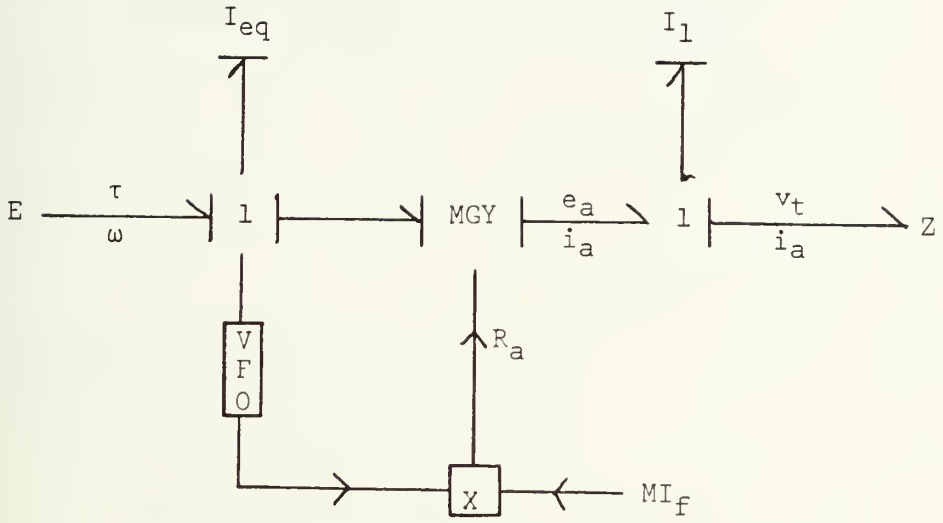

In this model the inertia of the rotating mass has been included and is shown connected to the -1 junction of the alternator. Now the causality required for the prime mover can be determined.

The I element imposes the velocity at the 1 junction so that the following causality must be imposed.

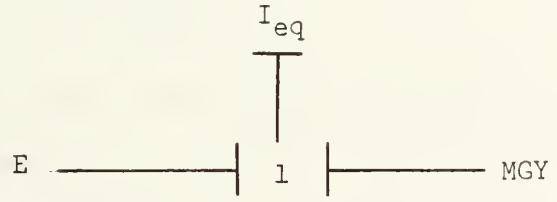

This requires that the prime mover be modeled as some type of torque source. This is as expected because if a velocity source were assumed, step changes in the input would impose a step change in the velocity of the rotating mass and to do so would require infinite power. As a result the model of the gas turbine must be of a form such that velocity is the

input signal and torque is the output signal.

From the simplified model bond graph the state variable representation can be formulated from the following equations.

$$\frac{d\omega_e}{dt} = \frac{1}{I_{eq}}(\tau_s - \tau_l) \qquad e = R\omega$$

$$\frac{di}{dt} = \frac{1}{I_l}(e - v) \qquad \tau = Ri$$

$$R = MI_f \cos \omega t$$

$$v = Zi$$

This model involves five parameters.

I_{eq} ≡ inertia of rotating masses

I_l ≡ synchronous reactance of alternator

M ≡ this parameter is defined above as $N_a N_f P$. However, it is closely approximated by the slope of the air gap voltage line of the alternator at synchronous speed.

$e = [MI_f(\cos \omega t)]\, \omega$

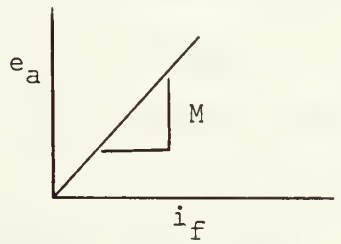

ω = constant

I_f ≡ field current, for the initial simulation will be assumed constant.

Z ≡ connected load.

The Analog setup sheet is shown on page 57 where the load Z is replaced by the induction motor model.

4.4 INDUCTION MOTOR A commonly used induction motor equivalent circuit is the Steinmetz equivalent circuit shown below.

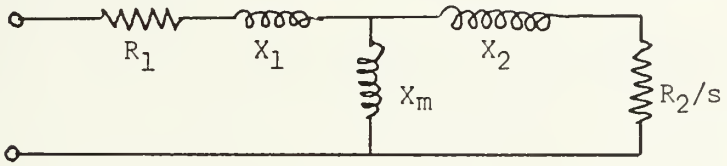

The derivation of this equivalent circuit is given in standard Electrical Engineering texts. This model can be simplified considerably without serious error by neglecting the magnetizing reactance X_m. The circuit can then be simplified to the following.

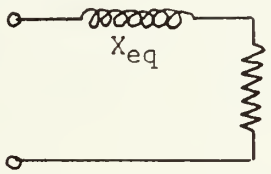

$$X_{eq} = X_1 + X_2$$

$$R_{eq} = R_1 + \frac{R_2}{s} \quad \text{and} \quad R_1 \sim R_2$$

Except at standstill $R_{eq} \sim R_2/s$. In the case of the wound rotor induction motor large resistance is added to the rotor circuit for starting so that through the entire operating range the equivalent resistance is $R_{eq} \sim \frac{R_2'}{s}$ where $R_2' = R_2 + R_{added}$.

For the case of the prototype motor, the added resistance is approximately thirty times as large as R_2 and is shunted out in four steps so that R_1 can be neglected at all speeds.

By applying a power balance across the air gap and neglecting losses an expression for the developed torque can be derived.

$$\tau_m = \frac{q I_2^2 \, R_2'}{\omega_s \quad s}$$

where (ω_s) is the synchronous mechanical speed and (q) is the number of phases.

4.5 PROPELLER The torque relationship for any non-cavitating propeller can be represented by an equation of the form

$$\tau = \rho D^3 n^2 C_\tau (\beta)$$

where the water density (ρ) and diameter (D) are constants. The torque coefficient $C_\tau(\beta)$ is a function of the velocity angle (β) where β is defined as $\beta = \tan^{-1}(V_Q/V_w)$ where V_Q is the axial velocity of flow through the propeller and

V_ω is the tangential velocity of the propeller at the maximum diameter. The angle β is identical to the propeller advance ratio (J) used in propeller design by naval architects where $J = Vo/\pi nD$. With β constant the propeller can be modeled by an expression of the form

$$\tau = K_p n^2$$

From the picture of the propeller shown in Figure 7, it is seen that the propeller operates in a nozzle with an axial length approximately one-half diameter. With this nozzle the flow rate through the propeller is of the approximate form $V_Q \propto Q/D^2$

$$V \propto n$$

As a result the velocity angle β becomes

$$\beta = \tan^{-1}\left(\frac{n}{\pi nD}\right) = \text{const}$$

The torque expression given above then reduces to the form commonly used to represent propeller loads over a wide range of RPM where torque is taken as directly proportional to RPM squared.

The prototype system was operated with the ship tied to the pier when the data was taken. Although there is some slight motion of the ship during the operation of the bow thruster it was assumed that the

propeller is stationary and that the axial velocity of water through the propeller is due to water motion only.

4.6 BEARING RESISTANCES All bearing resistances will be neglected in the simulation. In the case of the alternator where the speed deviations are slight the bearing drag is constant and will have no significant influence. For the induction motor the resistance will vary, but the resistance effects are assumed to be small compared to the load and driving torques. The resistances can therefore be neglected with no serious error.

5.1 PARAMETER ESTIMATES The system model to be used for this simulation requires values for the following parameters:

I_1 - engine inertia

I_2 - accessory drive inertia

I_3 - speed reducer inertia

I_4 - alternator inertia

X_{sa} - synchronous reactance of the alternator

X_{sm} - synchronous reactance of the induction motor

R_a - rotor resistance of motor

R_a' - added series rotor resistances

I_m - motor inertia

K_τ - engine torque/fuel flow ratio

- governor parameters

Where possible these parameters were obtained from information supplied by the equipment manufacturers. However, in some cases it was necessary to estimate parameters.

I_1 The engine inertia is divided into three parts, the compressor, turbine and accessory drive package. Estimates for compressor and turbine inertias were obtained from Solar.

Compressor	1.750 in-lb-sec^2
Turbine Stage (1)	.532
Turbine Stage (2)	.564
Turbine Stage (3)	.916
	3.762 in-lb-sec^2 at 22,300 RPM

$\underline{I_2}$ The accessory drive is approximated as follows. The idler gear and output gear are the largest rotating parts at the intermediate speed. These are approximated as steel discs one-half inch thick and eight inches in diameter. For a single disc,

$$I = \tfrac{1}{2}mr^2$$

$$m = \frac{\pi D^2 T \rho}{49} \qquad \text{where for steel } \rho = 487 \text{ lb/ft}$$

$$m = \frac{\pi(64)\ 487}{4(2)\ 1728 \cdot 384} = 0.0184 \text{ lb-sec}^2/\text{in}$$

$$I = \tfrac{1}{2}mr^2 = 0.147 \text{ in-lb-sec}^2$$

For two discs and considering the remaining parts as having the same inertia as a single disc, the total inertia of the accessory drive is approximately 0.5 in-lb-sec^2 at 6010 RPM.

$\underline{I_3}$ The speed reducer inertia is estimated by assuming that all inertias are negligible except that of the first-stage ring gear. Since all inertias will be referred to the output speed, both speed ratios and WR^2 values must be considered. The first-stage ring gear is approximated by a one-quarter inch steel disc eleven inches in diameter plus a ring two inches wide by one-quarter inch thick and eleven inches in diameter. The resulting inertia is approximately 1.0 in-lb-sec^2. Although the inertias of the second-stage parts are of the same order of magnitude as the first stage ring gear, they become insignificant compared to the first stage parts when referred to the output speed.

$\underline{I_4}$ The alternator rotor inertia was given on the manufacturer's drawings.

$$WR^2 = 951 \text{ lb-ft}^2 \quad \text{or} \quad I = 29.6 \text{ lb-ft-sec}^2$$

All inertias can now be referred to the output speed of 1200 RPM.

$$I_{1_{EQ}} = I_1 \left(\frac{N_{turb}}{N_{alt}}\right)^2$$

$$= \frac{3.76}{12} \left(\frac{22{,}300}{1200}\right)^2 = 108 \text{ lb-ft-sec}^2$$

$$I_{2_{EQ}} = I_2 \left(\frac{N_{acc\ drive}}{N_{alt}}\right)^2$$

$$= \frac{0.50}{12} \left(\frac{6010}{1200}\right)^2 \simeq 1 \text{ lb-ft-sec}^2$$

$$I_{3_{EQ}} = I_3 \left(\frac{N_{1st\ stage}}{N_{alt}}\right)^2$$

$$= \frac{1.0}{12} \left(\frac{6010}{1200}\right)^2 \simeq 2 \text{ lb-ft-sec}^2$$

$$I_{4_{EQ}} = I_4 = 29.6 \text{ lb-ft-sec}^2$$

It is seen that the inertias of the engine and the alternator are the dominant terms. The total inertia is taken as 140 lb-ft-sec^2.

$\underline{X_{sa}}$ The alternator synchronous reactance is given on General Electric drawings as 1.19 ohms. For a line frequency of 60 Hz;

$$L = \frac{X_{sa}}{\omega} = 0.00316\text{h}$$

$\underline{X_{sm},\ R_a}$ The motor reactance can be estimated from the equivalent circuit model used for the motor and the motor performance curves.

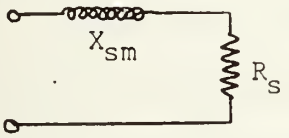

$$R_s = \frac{r_2}{s} \quad ; \quad s = \frac{N_s - N}{N_s}$$

From performance curves at the motor rating point:

N = 1180 RPM

I = 440 amps s = 1.66%

E = 440 volts

For the equivalent circuit used, the magnitudes of the phasor quantities are related by:

$$I = \frac{E}{Z} \quad \text{where} \quad Z = (R_s^2 + X_x^2)^{\frac{1}{2}}$$

$$X_s = 0.71 \text{ ohm}$$

$$Z \simeq \frac{E}{I} = 1 \text{ ohm} \quad \text{and} \quad L = 0.00188\text{h}$$

The rotor resistance is given in the General Electric drawings as 0.0117 ohms.

$\underline{I_m}$ No figures were available in the manufacturer's drawings for the motor inertia. The inertia was estimated from a drawing of the rotor where the mass was approximated by a steel right circular cylinder fifteen inches long by twenty inches in diameter. The inertia estimate is 14.1 lb-ft-sec^2. This is approximately fifty percent the inertia of the alternator and is a reasonable estimate.

The propeller is approximated by a steel disc four feet in diameter and one inch thick. This gives a value of 30 lb-ft-sec^2. When this inertia is referred to the motor speed through a speed ratio of approximately 2:1 the equivalent inertia of the propeller becomes 7.5 lb-ft-sec^2.

$\underline{K_T}$ The ratio of steady state engine torque to fuel flow is obtained from the engine performance curves. For constant speed and constant ambient conditions the torque is linear with fuel flow throughout the operating range. In this study where fuel input is not observed it is not necessary to isolate this constant from the overall gain in the engine control loop. In scaling of the simulation it is shown that where torque and fuel actuator angle are considered in non-dimensional form this constant is reduced to unity.

K_p No information on the propeller was available from the manufacturer. However, for the assumed propeller model which is

$$\tau_p = K_p N^2$$

a torque coefficient can be fit from the observed propeller performance. Using the maximum observed propeller speed for fitting the coefficient gives the following: N_{max} = 1125 RPM

Neglecting frictional losses the motor torque at this speed is 1370 lb-ft so that

$$K_p = \frac{\tau_p}{N^2}$$

$$= 0.00108 \text{ lb-ft/RPM}^2$$

GOVERNOR SETTINGS There are five parameters connected with the engine governing system. These parameters can vary over a wide range depending on the governor settings. In order to determine the exact settings it would be necessary to measure the open loop frequency response of the control system. The ranges of the governor settings as well as nominal values were supplied by the Woodward Governor Company. The nominal values will be used in this study. The feedforward gain and loop gain will be varied and the effect on system performance observed. The values for the other parameters will be taken as follows:

Parameter	Range	Nominal Value
α_1	23 to 184	28
α_2	--	1.6
α_3	0.08 to 160	4
K	vary in simulation	30,000
α	--	10

Parameter	Range	Nominal Value
γ	--	46
σ	--	2210
Feed Forward Gain	vary in simulation	0.0045

R_a' The added rotor resistances are given in the manufacturer's drawing. The resistances are shunted out in four steps.

Step 1	.240 ohms/phase
Step 2	.088 ohms/phase
Step 3	.072 ohms/phase
Step 4	.063 ohms/phase

5.2 SIMULATION-ANALOG SET UP The models derived in previous sections can be set up for Analog computation in a straightforward manner. The set up for the complete system is shown in Figure 9 on page 57.

GAS TURBINE The Analog set up for the gas turbine and speed control is implemented directly from the block diagram of the engine on page 31.

(1) The feedforward of load disturbance is a high pass filter of the form:

$$\frac{Y}{X} = \frac{KS}{TS + 1}$$

This transfer function is realized by a circuit of the form below which is taken from reference (3).

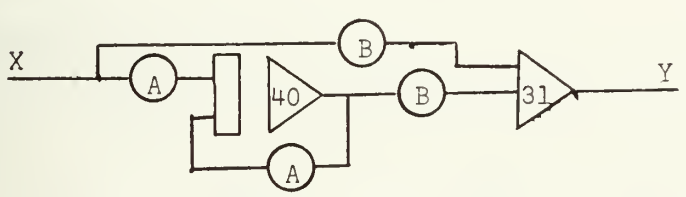

where A = 1/T

B = k/T

The operator is realized using A40 and A31 in the simulation.

(2) The engine speed is obtained at A60 by integrating the difference of the driving and load torques.

$$\Delta\omega = \frac{1}{I} \int_{t_0}^{t_1} (\tau_e - \tau_a)\, dt = \omega(t_1) - \omega(t_0)$$

Since $\omega(t_0)$ can be taken as the base speed of the alternator the output of A60 when properly scaled gives the error in engine speed. This voltage is summed with the output of the feedforward network to give the error signal developed in the EGA control box.

(3) The error signal is generated by A61.

$$E_1 = \frac{K_1 s}{T_s + 1} \bar{\tau}_a - K_2 \frac{\Delta\omega}{\omega_{ref}} \quad \text{where} \quad \bar{\tau}_a = \frac{\tau_{alt}}{\tau_{ref}}$$

(4) Since the operator representing the stabilizer section of the control box has been neglected the transfer function between the error signal E_1 and the output of the fuel actuator angle Θ is

$$\frac{\Theta}{E_1} = \frac{K_3 (T_1 s + 1)(T_2 s + 1)}{s (T_3 s + 1)}$$

This transfer function can be realized by taking two operators cascaded.

For $\frac{Y}{X} = \frac{T_1 s + 1}{s}$

$$\dot{Y} = T_1 \dot{X} + X$$

or $Y = T_1 X + \int X$

This operator is realized using A95, A39, and A01

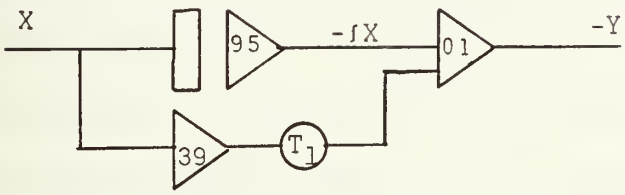

The operator for $\frac{Y}{X} = \frac{(T_2 s + 1)}{(T_3 s + 1)}$ is also from reference (3).

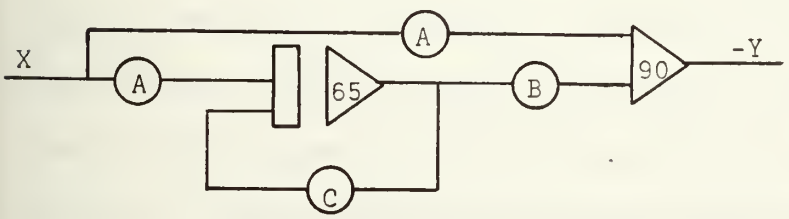

$A = K T_2/T_3$

$B = (T_2 - T_3)/T_2 T_3$

$C = 1/T_3$

The output of A90 represents the angle of the fuel control actuator. In the derivation of the turbine model it was shown that except for a transport delay the torque is proportional to fuel input. The fuel control

angle is assumed proportional to fuel input. The engine dead time can be neglected so that except for a gain factor the output of A90 represents the gas turbine torque.

With the correct setting on P60 the output of A91 represents engine torque.

The gas turbine model is now complete except for the load torque. The alternator torque is generated by the multiplier A38. This torque is of the form

$$\tau = \tau_0 (1 + \cos 2 \omega t)$$

It is necessary to filter the double frequency component for two reasons.

(1) The pulsations are a form of noise which cause slight variations in engine speed. When compared to the base engine speed of 1200 RPM, these fluctuations in speed are insignificant. However, with a fine speed control on the engine where the variations in speed due to the real load changes are of the order of 10 RPM, the noise from the load torque signal becomes significant. This point is most evident when scaling the integrator which generates the speed signal. If the integrator is scaled so that the output is N/N_{ref} where N_{ref} is 1200 RPM the integrator gain which represents the reciprocal of inertia is small and corresponds to a large inertia. In the simulation it is necessary to generate N/N' where N' is of the order of the maximum deviation in engine speed due to changes in load torque. As a result, the integrator gain is increased to the point where the double frequency torque pulsations are passed along with the D.C. torque level.

(2) It is also necessary to filter the load torque because it is input to the load sensing network which has a derivative action.

A low pass filter was chosen over a band stop filter for removing the torque pulsations because the low pass filter requires less Analog hardware. An attenuation of 40 db at the noise frequency will provide adequate filtering. At this level the noise is barely noticeable on the oscilloscope. A first order filter tuned for an attenuation of 40 db at the noise frequency of 120 Hz will have its break point at 1.2 Hz and is considered to be too low for the expected load transients. As a result a second order filter was used with the break point at 12 Hz, and 40 db attenuation at 120 Hz. The transfer function of the second order filter is of the following form:

$$G(jw) = \frac{1}{1 + 2\zeta\left(\frac{j\omega}{\omega_n}\right) + \left(\frac{j\omega}{\omega_n}\right)^2}$$

With the break point at 12 Hz and with ζ set at 0.55 in order to minimize overshoot near the break frequency, the transfer function becomes:

$$G(s) = \frac{Y}{X} = \frac{1}{1 + \frac{1.1}{7.5}s + \frac{s^2}{75^2}} \quad \text{where } s = jw$$

Performing the operations indicated gives

$$\ddot{Y} = 5650X - 82.5\,\dot{Y} - 5650Y.$$

Scaling this equation to a form suitable for Analog computation gives

$$\left[\frac{\ddot{Y}}{100}\right] = 56.5X - 82.5\left[\frac{\dot{Y}}{100}\right] - 56.5Y.$$

This filter is shown on the Analog set up sheet using A70, A74 and A100.

ALTERNATOR, INDUCTION MOTOR, PROPELLER The equations representing these components were derived previously.

(1) $\frac{d\omega}{dt} = \frac{1}{I_1} (\tau_e - \tau_a)$

(2) $R = MI_f \cos \omega t$

(3) $\tau_a = R_i$

(4) $\frac{di}{dt} = \frac{1}{(L_a + L_m)} (e - v)$

(5) $e = R\omega$

(6) $v = \frac{iR_2}{s} = i \left[\frac{R_2\omega_0}{\omega_0 - \omega}\right] = iR_2 \left[\frac{N_0}{N_0 - N}\right]$

(7) $\tau_m = i \left[\frac{iR_2}{s}\right] = iv$

(8) $\tau_p = KN^2$

(9) $\frac{dN}{dt} = \frac{30}{(I_p + I_m)\pi_1} (\tau_m - \tau_p)$

Equation (1) has been described above with A60 generating the alternator speed.

Equation (2) determines the gyrator modulus of the alternator and is a function of the field current and frequency. In the prototype the speed variations were insignificant compared to the base speed so that the frequency can be considered constant. Although the field current did vary slightly a constant field current will be used. The gyrator modulus is then of the form

$R = K \cos (\omega t)$

The 60 Hz sinusoidal waveform was generated using the Wavetek signal generator.

Equation (4) is solved using A00 where e is the air gap voltage of the alternator and v is the back emf of the induction motor.

Equation (5) is the air gap voltage of the alternator. With the assumption of constant frequency and field current, e is a sinusoidal voltage of constant frequency and amplitude.

Equation (6) generates the back emf of the induction motor and is realized at multiplier A03.

Equation (7) generates the torque output of the induction motor. This torque also contains a double frequency component. However, since the induction motor speed is scaled to the 1200 RPM synchronous speed it is not necessary to filter this torque.

Equation (8) is realized at multiplier A63 where the propeller torque coefficient is set on P67.

The switching of the induction motor rotor resistances is set up in the network which is input to the junction inverter A04. The values of the switched resistors are set on the potentiometers P95, P00, P32, and P65 with the residual resistance on P03. The switched resistors are input to the amplifier junction of A04 through the D/A switches shown. The switching of the D/A switches is controlled by the logic outputs of the comparators.

In the prototype system the switching is controlled by time delay relays. This switching action is simulated in the following way. A05 generates a ramp timing signal. This signal is input to comparators C04, C34, C64, and C94. These comparators have a negative bias corresponding to the time at which switching is to occur. The inverted logic output of each comparator is input to the switch control of the respective D/A switch. Initially the output of A05 is zero. All comparators are in the

low position. As a result, the inverted output to the D/A switch is high and all switches are conducting. The input to A04 is

$$i\ (R_a + R_1 + R_2 + R_3 + R_4).$$

As the output of A05 increases to a level above the bias of each comparator, switching occurs when the comparator logic output goes high and the inverted output goes low so that the respective D/A switches are turned off. After all switching occurs, only the resistance due to P03 remains in the circuit.

ANALOG DIAGRAM Fig 9.

——— ANALOG PATCHING

▬▬▬ LOGIC PATCHING

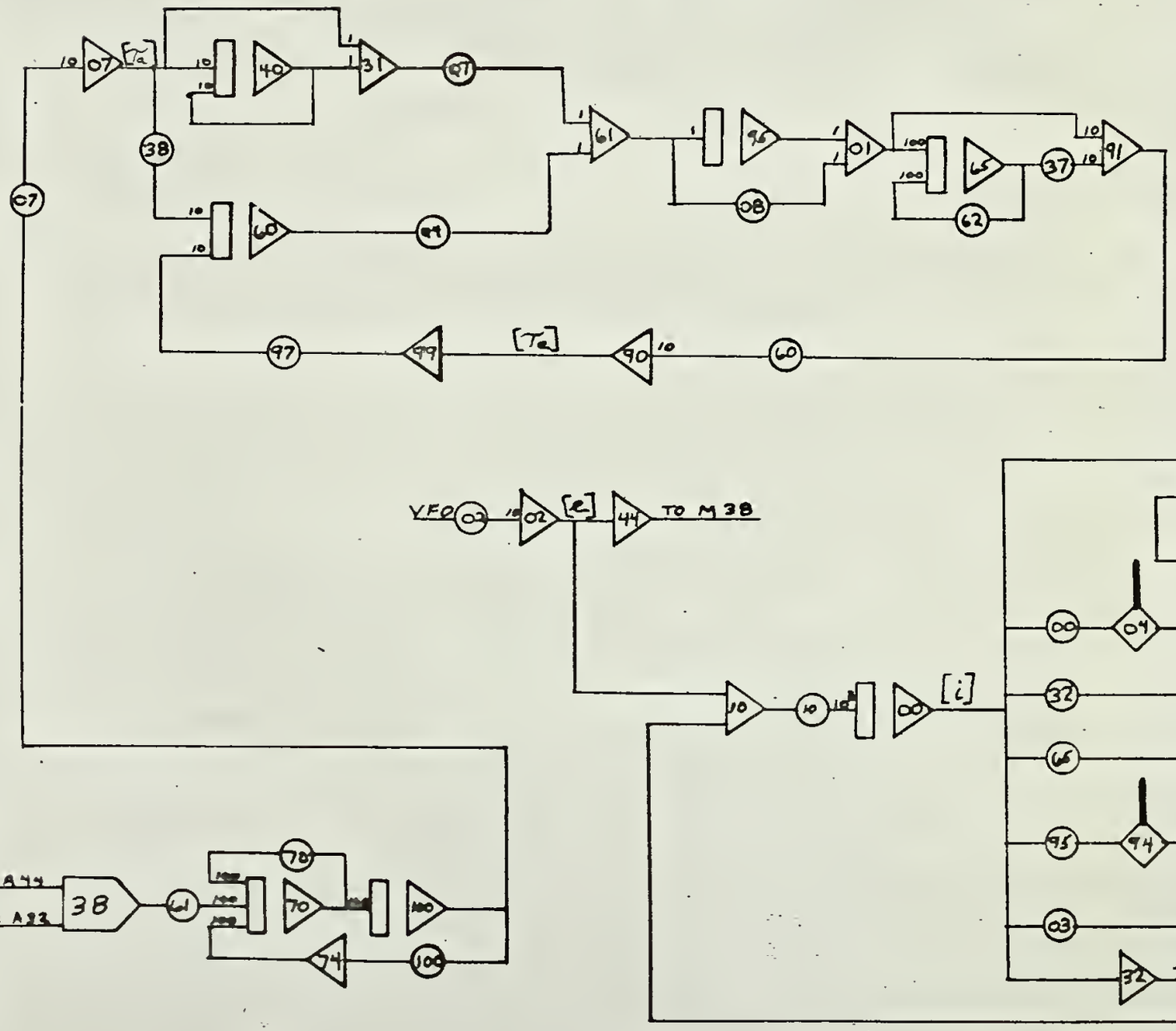

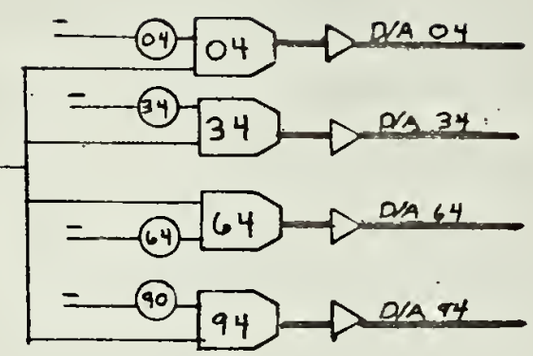

5.3 SCALING ANALOG SIMULATION

GAS TURBINE When nominal values are substituted for the governor settings the block diagram for the prime mover and governor is as shown below.

Figure 13.

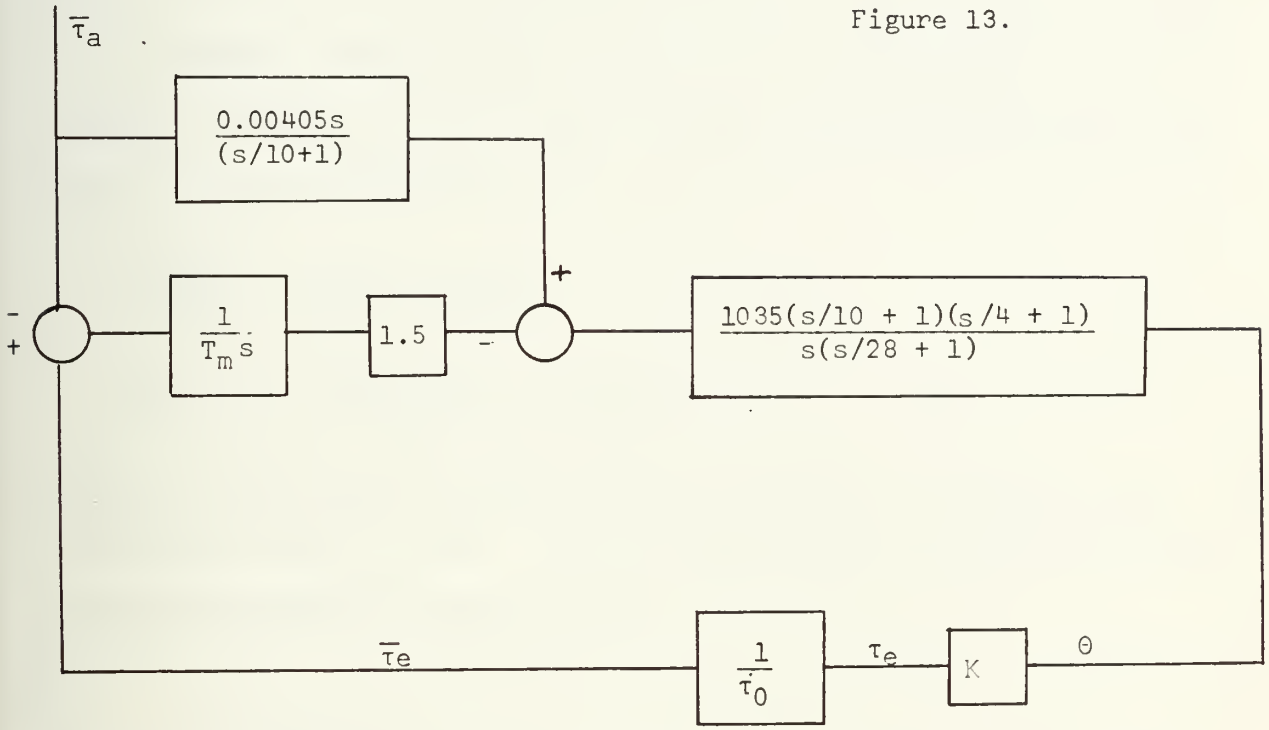

The machine time constant (T_m) is defined from the non-dimensional equation for the alternator speed.

$$\frac{\tau_e - \tau_a}{\tau_0} = \left(\frac{I\omega_0}{\tau_0}\right) \frac{d}{dt} \left(\frac{\omega}{\omega_0}\right) \qquad \text{where } T_m = \frac{I\omega_0}{\tau_0}$$

The base speed ω_0 is 125.6 rad/sec and the inertia I is the combined inertia of the engine, speed reducer and alternator referred to ω_0. The selection of the base torque is somewhat arbitrary. Based on the engine power rating of 1200 HP with output at 1200 RPM the base torque is:

$$\tau_0 = \frac{1200 \times 550}{125.6} = 5250 \text{ lb-ft}$$

The maximum expected steady load torque is approximately 1500 lb-ft. The

maximum engine torque is limited by the acceleration limiting response of the fuel control valve. For a step load change of 1500 lb-ft the maximum engine torque developed is assumed to be 3000 lb-ft. With this base torque the engine time constant is 5.86 sec. The corresponding gain on the integrator which generates $\Delta\omega$ is 0.170. The expected maximum deviation in speed is taken to be 7.5 rad/sec. With this base speed the gain on the speed integrator is:

$$\left[\frac{\Delta\omega}{7.5}\right] = \frac{1}{T_m's} \quad \frac{\tau_e - \tau_a}{\tau_0}$$

where $T_m' = \frac{140 \times 7.50}{3000} = 0.352$ sec

The gain on the speed integrator must be increased by a factor of 16.7 for this new value of of T_m'. This is accomplished by modifying the system transfer function as shown below.

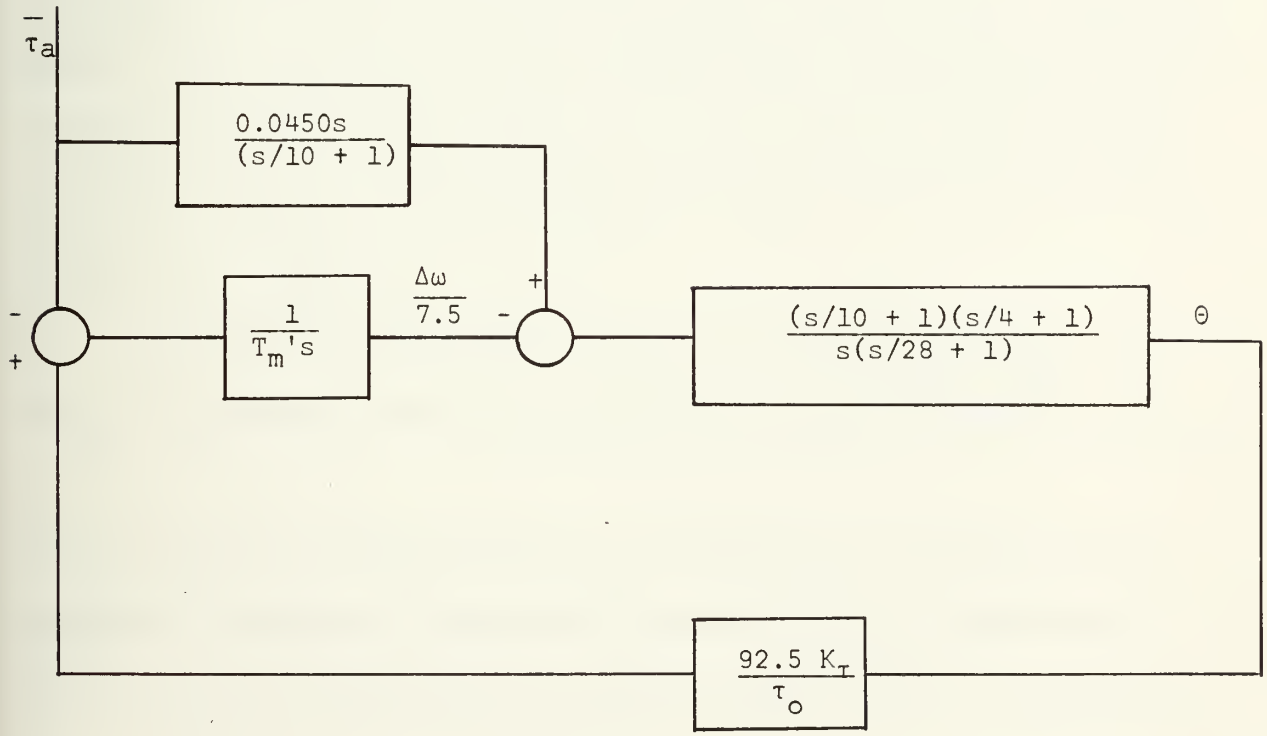

The operator $\frac{1}{T_m's}$ is generated by A60. The scaled equation is*

$$\left[\frac{\Delta\omega}{7.5}\right] = \frac{10(2840)}{s}\left[\frac{\tau_e - \tau_a}{3000}\right]$$

with the pot settings on P38 and P97.

The scaled feedforward transfer function with T = 10 and K = 0.1 is generated at A40 and A31. The gain of the feedforward is then set on Q07.

The operator $\frac{(s/4 + 1)}{s}$ is generated at A01. For $T_1 = 4$ the setting on P08 is 2500.

The operator $\frac{K(s/10 + 1)}{(s/28 + 1)}$ is generated at A90. In order to reduce the number of pots required K is taken as $100T_3/T_2$. With $T_2 = 1/10$ and $T_3 = 1/28$ the pot settings and gains are:

P62 = 100(2800)

P37 = 100(1800)

The inputs to A65 and A91 from A01 are then at a gain of 100. Since the gain of 100 is difficult to obtain at the input to summer A91 the output of A91 is scaled down by a factor of 10. The inputs and output of A91 are then as shown on the Analog diagram, Figure 9. The output of A91 corresponds to $10\,\frac{T_3}{T_2}\,\theta$.

The loop gain is introduced at A90. With $K = \frac{\theta}{\theta_{max} - \theta_{min}}$ and $\theta_{max} - \theta_{min}$ taken as 30° the required gain at P60 is determined as shown

* The following convention is used to represent all scaled equations: normalized variables in machine units are in brackets, potentiometer coefficients are in parentheses and amplifier gains before the parenthesis.

below.

$$\overline{\tau}_e = \frac{92.5\ K_\tau \Theta}{\tau_0} = \frac{92.5\Theta}{\Theta_{max} - \Theta_{min}}$$

The output of A91 is $10\ \frac{T_3}{T_2}\ \Theta$

$$10\ \frac{T_3}{T_2}\ (\text{gain})\ \Theta = \frac{92.5\ \Theta}{\Theta_{max} - \Theta_{min}}$$

$$(\text{gain}) = \frac{92.5\ T_2}{T_3(\Theta_{max} - \Theta_{min})} = .8650$$

The required setting on P60 is then 1(8650).

LOAD COMPONENTS The induction motor speed is generated at A35. The unscaled equation is:

$$N = \frac{30}{\pi I s}\ (\tau_m - \tau_p)$$

The maximum motor speed is 1200 RPM which is the synchronous speed. The maximum steady motor torque is approximately 1500 lb-ft. Since the simulated motor torque has the double frequency component the maximum torque is twice the instantaneous D.C. level. As a result the maximum torque is taken as 4000 lb-ft. With the inertia (I) taken as 21.6 lb-ft-sec^2 the scaled equation becomes:

$$\left[\frac{N}{1200}\right] = \frac{10(1475)}{s}\ \left[\frac{\tau_m - \tau_p}{4000}\right] \qquad \text{Set on P35}$$

The propeller torque is generated at A63. The unscaled equation is:

$$\tau_p = K_p N^2$$

With $K_p = 1.08 \times 10^{-3}$ and the torque and speed base values as above the scaled equation becomes:

$$\left[\frac{\tau_p}{4000}\right] = 1(3880)\ \left[\frac{N^2}{1.44 \times 10^6}\right] \qquad \text{Set on P67}$$

The voltages and current in the simulation must be scaled based on peak values rather than the RMS values. For maximum RMS values of 440 volts and I/phase of 1000 amps the base values are taken as:

I_{base} = 1414 amps

V_{base} = 750 volts

Multiplier A33 generates the unscaled product of e and i. This is scaled to the induction motor torque as follows. For the induction motor for three phases:

$$P(t) = 3\ V_{max} \sin(\omega t)\ I_{max} \sin(\omega t + \phi)$$

or

$$\tau_m(t) = \frac{3\ V_{max} I_{max}\ (1 + \cos 2\omega t)}{2\omega_s}$$

where the phase angle can be neglected in scaling the equation and (.7376) is a conversion from newton-meters to lb-ft. ω_s is the synchronous mechanical speed which for this case is 125.6 rad/sec. With the base variables assumed above the scaled equation becomes:

$$\left[\frac{\tau_m}{4000}\right] = 10(2340)\left[\frac{v}{750}\right]\left[\frac{i}{1414}\right]$$ Set on P36

The output of A00 must be scaled to I_{max} = 1414. The unscaled equation for A00 is:

$$i = \frac{1}{s}\frac{(e - v)}{L}$$

Using the base values for current and voltage and the equivalent inductance (L) for a single phase the scaled equation is:

$$\left[\frac{i}{1414}\right] = \frac{10^3\ (8460)}{s}\ \left[\frac{e - v}{750}\right]$$

The motor voltage is generated at A03. The unscaled equation is:

$$v = \frac{R_a I N_S}{N_S - N} = \frac{RI}{1 - N/N_S}$$

The denominator is generated at A06 and is already in a non-dimensional form. Scaling the equation for current and voltage gives:

$$\left[\frac{v}{750}\right] = \frac{1.89\ R_a}{1 - N/N_s} \left[\frac{i}{1414}\right]$$

The potentiometers in the switching network are then set to 1.89 R_a and R_a' where R_a is the value for the rotor resistance and R_a' the value of the added rotor resistance.

The alternator torque is generated at multiplier A38. As shown above this output can be scaled to a base torque of 4000 lb-ft using the same setting as on P36 which is 10(2340). However, the alternator torque is filtered before being input to the gas turbine section so that it is not necessary to scale this signal for the double frequency pulsation. With the turbine base torque taken as 3000 lb-ft the gain on the output of A38 is 10(3100). Since the second order filter is set to a gain of (1) this gain is set on P07.

The scaled variables for all amplifiers and settings for all potentiometers are given on the assignment sheets given in Tables 1 and 2.

Table 1.

AMPLIFIER ASSIGNMENTS

Amplifier	Scaled Value	Comment
00	$i/1414$	
01		Governor Control Box
02	$e/750$	Alternator Modulus
03	$v/750$	I.M. Back emf
04	$1.89R_a i/1414$	For I.M. Back emf
05		Time Signal for Resistor Network
06	$(N_S-N)/N$	I.M. Slip
07	$\tau_a/3000$	
09	$v/750$	Invert I.M. Back emf
10	$(v-e)/750$	
14	$-(N_S-N)/N$	Invert A06
30		LPF for Viewing Torques
31		FFWD of Governor
32	$-i/1414$	
33	$vi/750 \times 1414$	I.M. Torque
34	$-N^2/1.44 \times 10^6$	
35	$N/1200$	I.M. Speed
36	$(\tau_p - \tau_m)/4000$	
38		Load Torque on G.T.
39		Governor Control Box
40		Governor FFWD Net

Amplifier	Scaled Value	Comment
44		Invert A02
60	$\Delta\omega/7.5$	Change in Alternator Speed
61		Governor Error Signal
63	$N^2/1.44 \times 10^6$	For Propeller Torque
65		Governor Control Box
70		Butterworth Filter
74		Butterworth Filter
90	$\tau_e/3000$	G.T. Torque
91		Fuel Control Angle
95		Governor Control Box
100		Butterworth Filter

Table 2.

POTENTIOMETER ASSIGNMENTS

POT	PARAMETER	SETTING W/GAIN
Q04	$\Delta\omega/\omega_0$ Gain	1000 (10)
Q07	FFWD gain	2000 (vary)
00	R_a (switched)	6000
02	Alt. modulus	Set for A07 output =.8500
03	R_a	0597
04	Switching time	1178
05	Timing signal	0500
07	Scale τ_a	3103 (10)
08	Cont. box setting	2287
10	Motor inductance	8277 (1000)
32	R_a (switched)	2000
34	Switching time	3291
35	Inertia of I.M.	2000 (10)
36	Scale motor torque	2341 (10)
37	Govt. Cont. box	1800 (10)
38	Alt. inertia	2841 (10)
60	Control loop gain	2177 (10) (vary)
61	Butterworth filter	5649 (100)
62	Govt. Cont. box	2661 (100)
64	Switching time	4895
65	R_a (switched)	2005
67	Scale propeller torque	3880
70	Butterworth filter	8243
90	Switching time	6819
95	R_a (switched)	2001
97	Alt. inertia	2841 (10)
100	Butterworth filter	5648 (100)

6. RESULTS

The results of monitoring the prototype performance and the results of the simulation are shown on pages 69 through 75. A chart speed of twenty-five millimeters/second was used for all recordings. Strips A-L correspond to a time duration of approximately fourteen seconds while channels M-BB span approximately the first eight seconds of the simulation. The records are presented in the following order.

A. Observed Alternator Speed Deviation

B. Simulated Alternator Speed Deviation

C. Observed K.W. Load (through 0.068 sec. LPF)

D. Simulated Alternator Torque (through 0.068 sec. LPF)

E. Observed Line Current

F. Simulated Line Current

G. Observed Induction Motor Speed (A.C. tachometer)

H. Simulated Induction Motor Speed

I. Simulated Motor Torque (through 0.068 sec. LPF)

J. Simulated Alternator Torque (through Butterworth filter)

K. Simulated Engine Torque - No Dead Time, No FFWD

L. Simulated Engine Torque - No Dead Time, With FFWD

M. Alternator Speed with FFWD Gain (Q07) at .1000

N. Alternator Speed with FFWD Gain at .2000

O. Alternator Speed with FFWD Gain at .3000

P. Alternator Speed with FFWD Gain at .5000

Q. Simulated Output of Governor Load Sensing Section

R. Simulated Governor Error Signal

S. Observed Alternator Terminal Voltage

U. Simulated Alternator Speed with 0.1 Sec. Dead Time

V. Simulated Engine Torque with 0.1 Sec. Dead Time

W. Simulated Fuel Control Angle with 0.1 Sec. Dead Time

X. Simulated Alternator Speed with 0.01 Sec. Dead Time

Y. Simulated Engine Torque with 0.01 Sec. Dead Time

Z. Simulated Alternator Speed - Loop Gain = 1.0 Per Unit

AA. Simulated Alternator Speed - Loop Gain = 1.6 Per Unit

BB. Simulated Alternator Speed - Loop Gain = 2.3 Per Unit

Figure 10

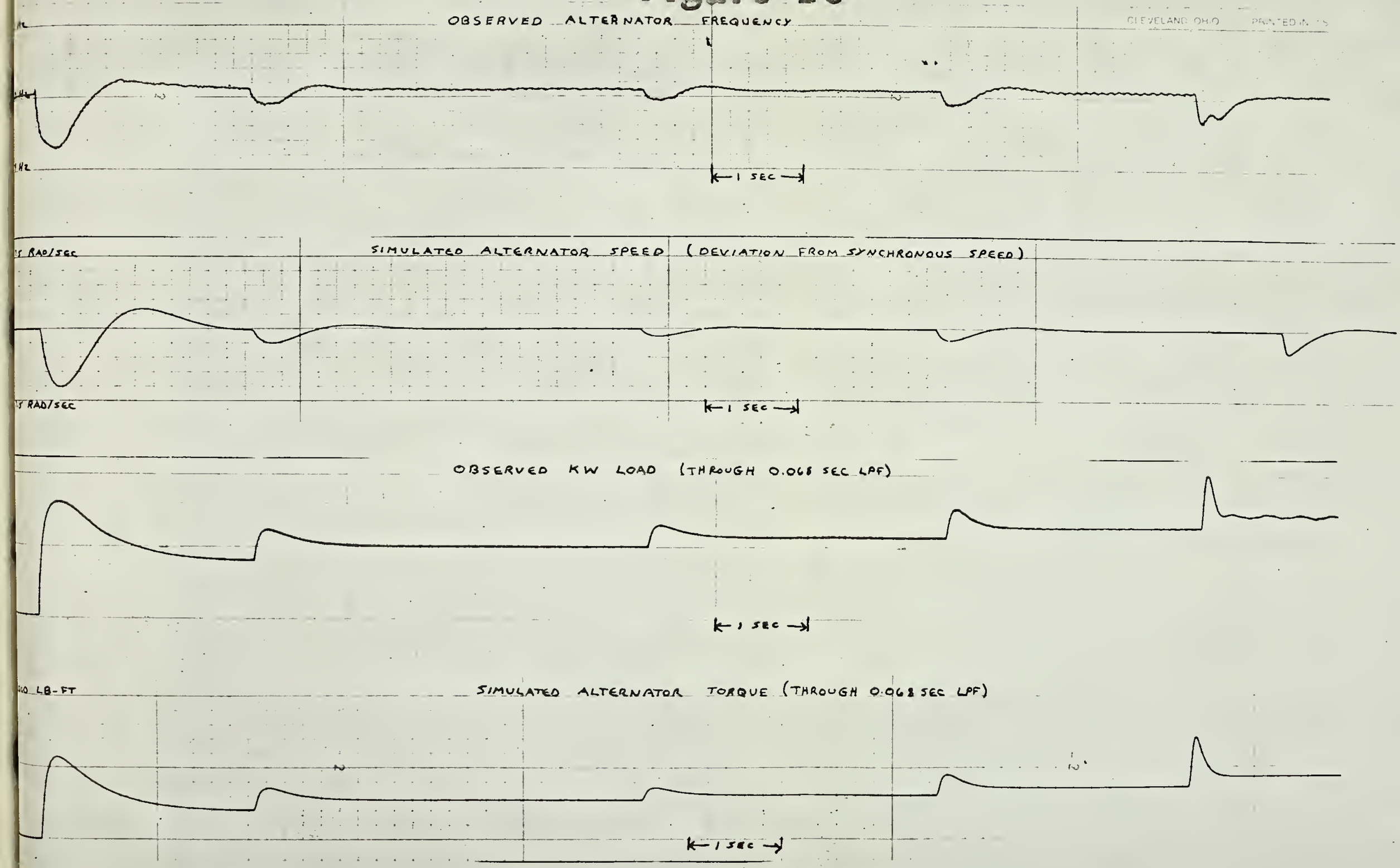
OBSERVED ALTERNATOR FREQUENCY
1 SEC
SIMULATED ALTERNATOR SPEED (DEVIATION FROM SYNCHRONOUS SPEED)
1 SEC
OBSERVED KW LOAD (THROUGH 0.068 SEC LPF)
1 SEC
SIMULATED ALTERNATOR TORQUE (THROUGH 0.068 SEC LPF)
1 SEC

Figure 10

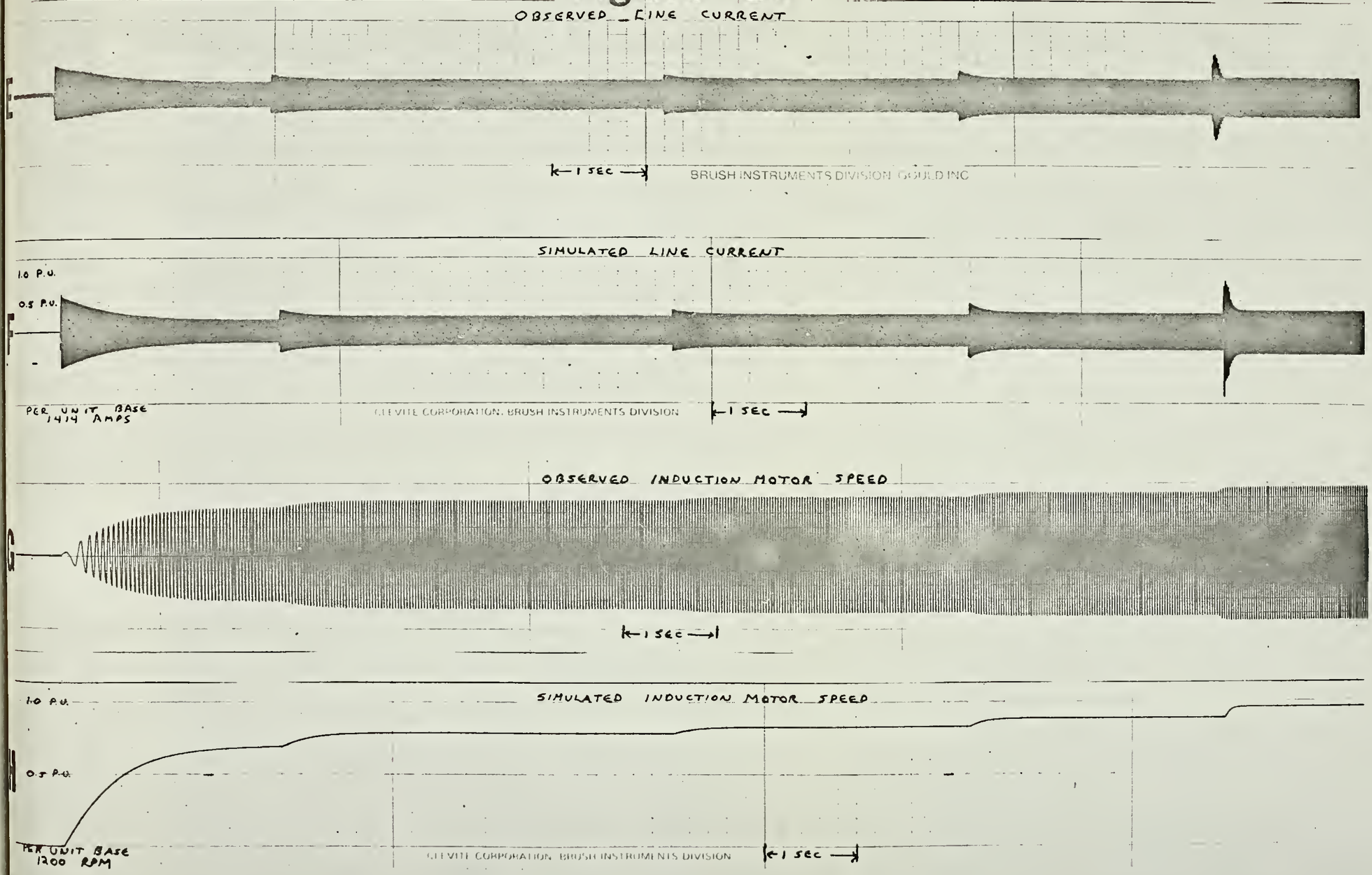
OBSERVED LINE CURRENT
← 1 SEC →
BRUSH INSTRUMENTS DIVISION GOULD INC
SIMULATED LINE CURRENT
1.0 P.U.
0.5 P.U.
PER UNIT BASE
1414 AMPS
CLEVITE CORPORATION, BRUSH INSTRUMENTS DIVISION
← 1 SEC →
OBSERVED INDUCTION MOTOR SPEED
← 1 SEC →
SIMULATED INDUCTION MOTOR SPEED
1.0 P.U.
0.5 P.U.
PER UNIT BASE
1200 RPM
CLEVITE CORPORATION, BRUSH INSTRUMENTS DIVISION
← 1 SEC →

Figure 10

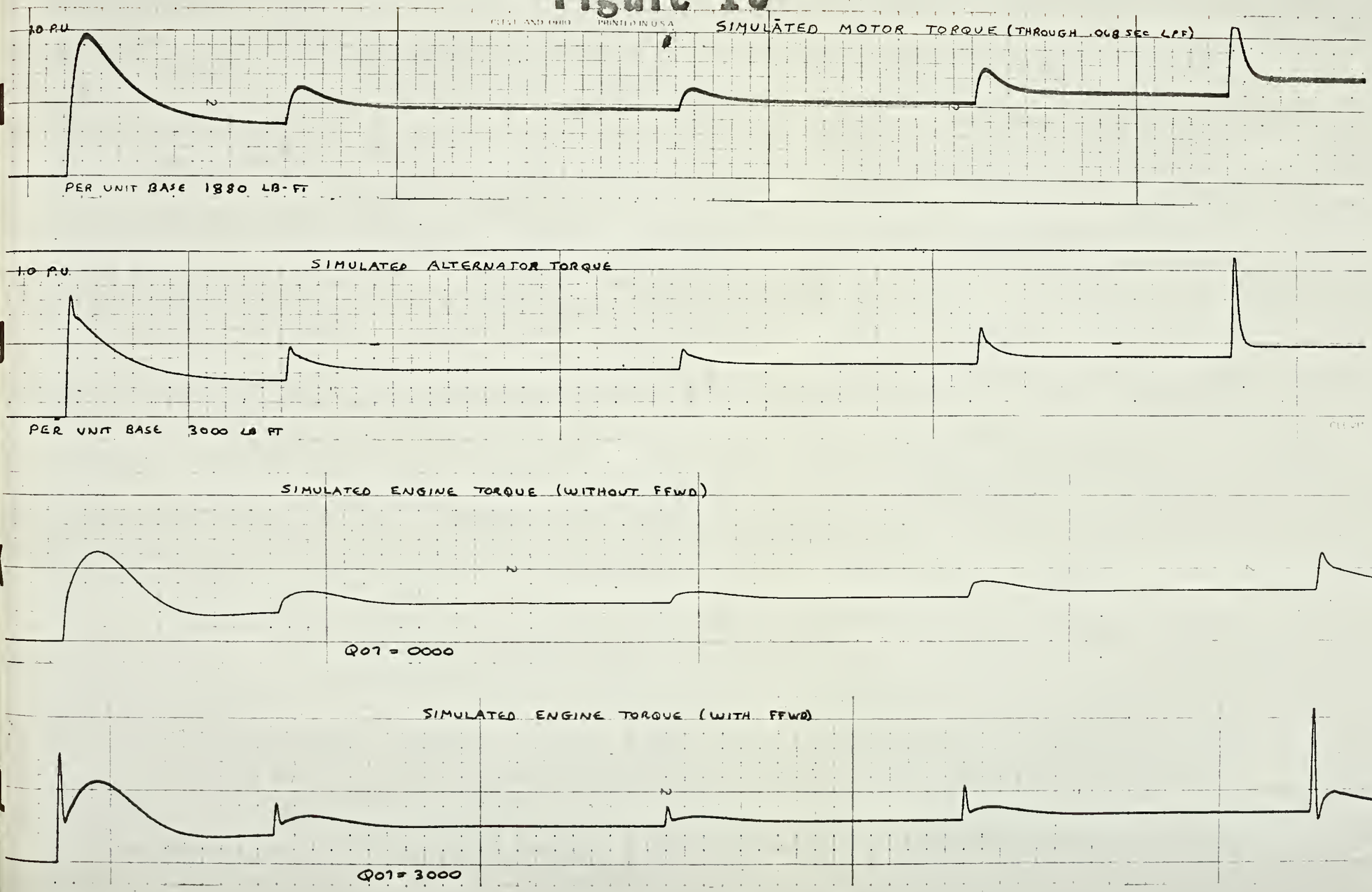
2.0 P.U.
SIMULATED MOTOR TORQUE (THROUGH .068 SEC LPF)
PER UNIT BASE 1880 LB-FT
1.0 P.U.
SIMULATED ALTERNATOR TORQUE
PER UNIT BASE 3000 LB FT
SIMULATED ENGINE TORQUE (WITHOUT FFWD)
Q01 = 0000
SIMULATED ENGINE TORQUE (WITH FFWD)
Q01 = 3000

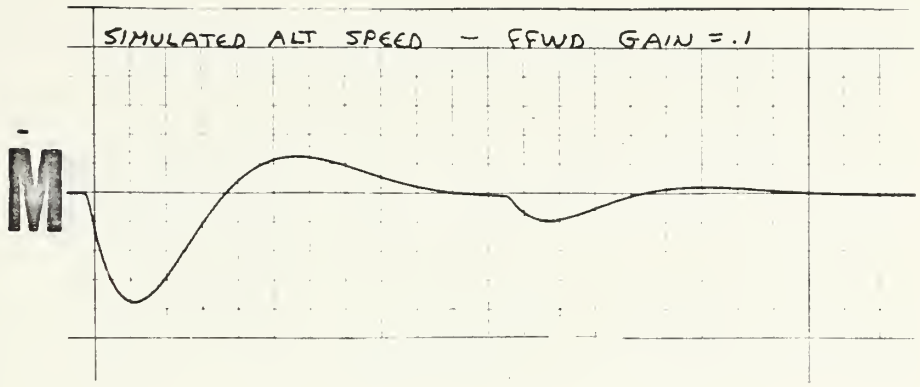
SIMULATED ALT SPEED - FFWD GAIN = .1
M

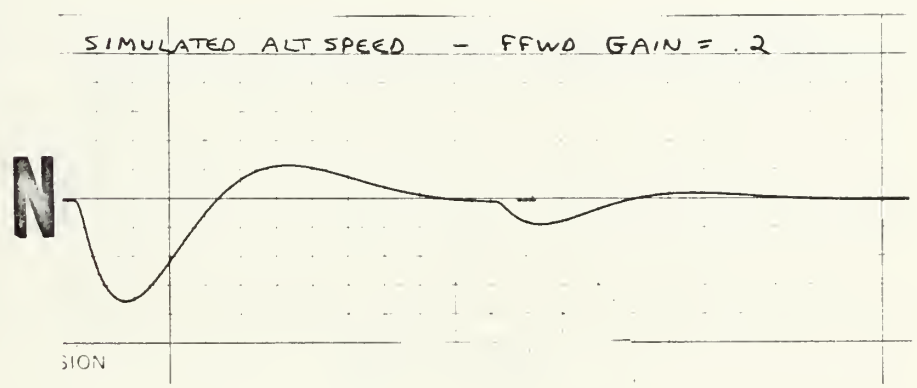
SIMULATED ALT SPEED - FFWD GAIN = .2
N

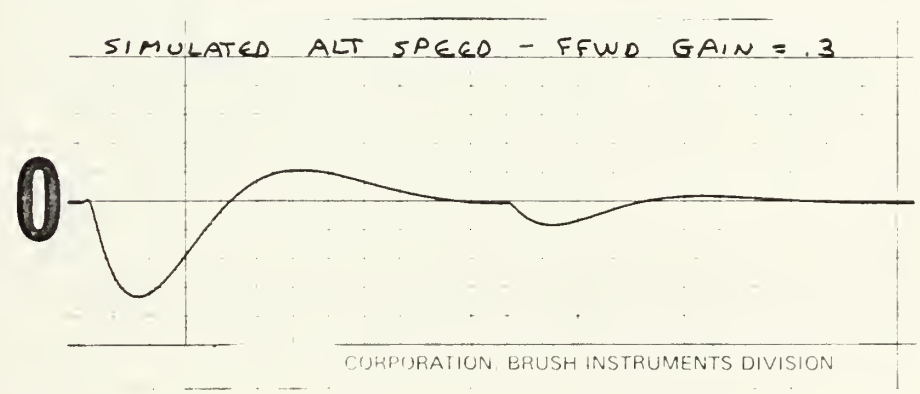
SIMULATED ALT SPEED - FFWD GAIN = .3
O
CORPORATION, BRUSH INSTRUMENTS DIVISION

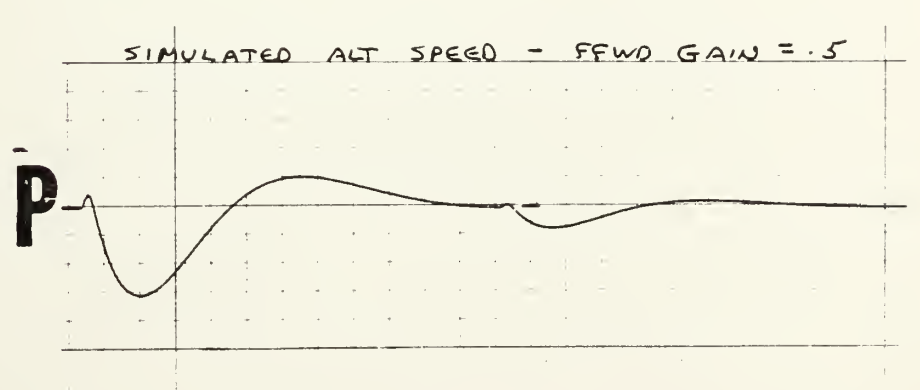
SIMULATED ALT SPEED - FFWD GAIN = .5
P

Figure 10.

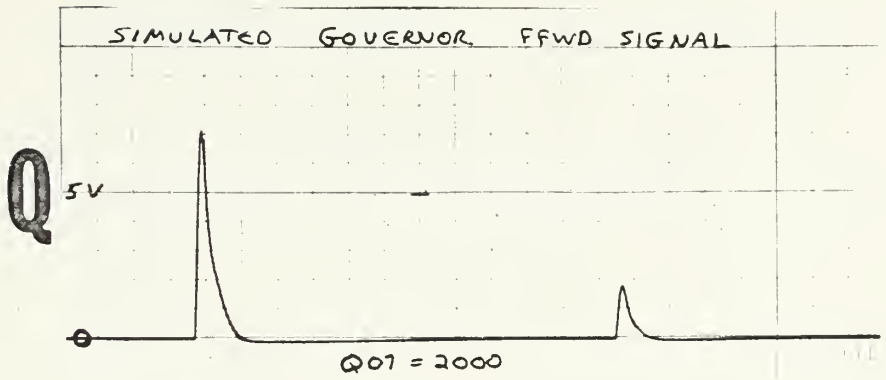

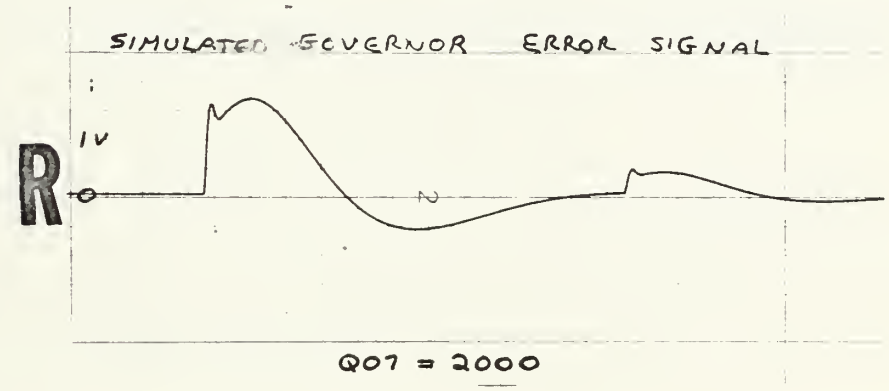

Figure 10.

o OBSERVED ALTERNATOR TERMINAL VOLTAGE

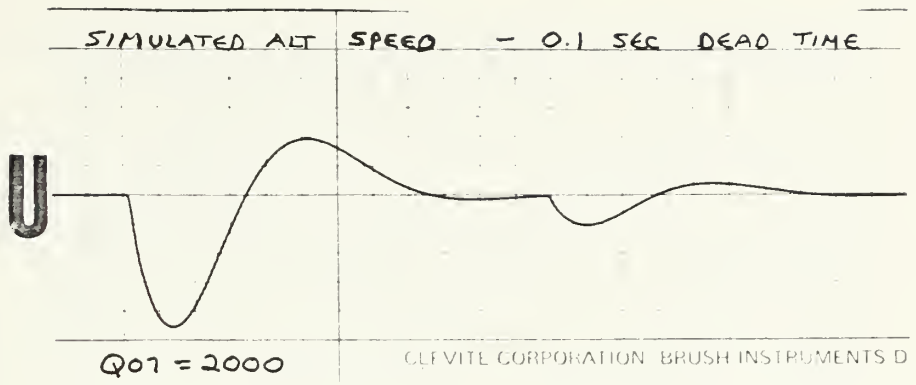
SIMULATED ALT SPEED - 0.1 SEC DEAD TIME
U
Q07 = 2000
CLEVITE CORPORATION BRUSH INSTRUMENTS D

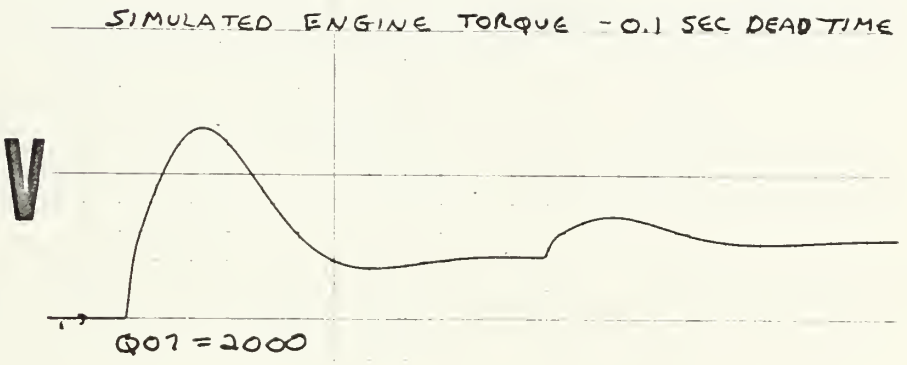
SIMULATED ENGINE TORQUE - 0.1 SEC DEAD TIME
V
Q07 = 2000

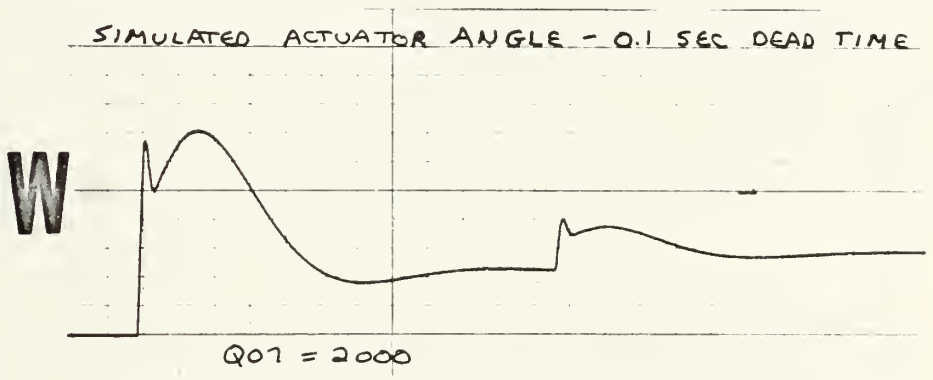
SIMULATED ACTUATOR ANGLE - 0.1 SEC DEAD TIME
W
Q07 = 2000

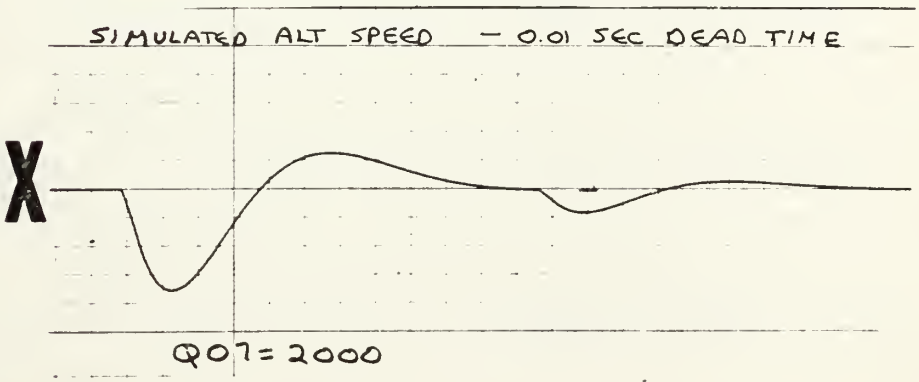
SIMULATED ALT SPEED - 0.01 SEC DEAD TIME
X
Q07 = 2000

Figure 10.

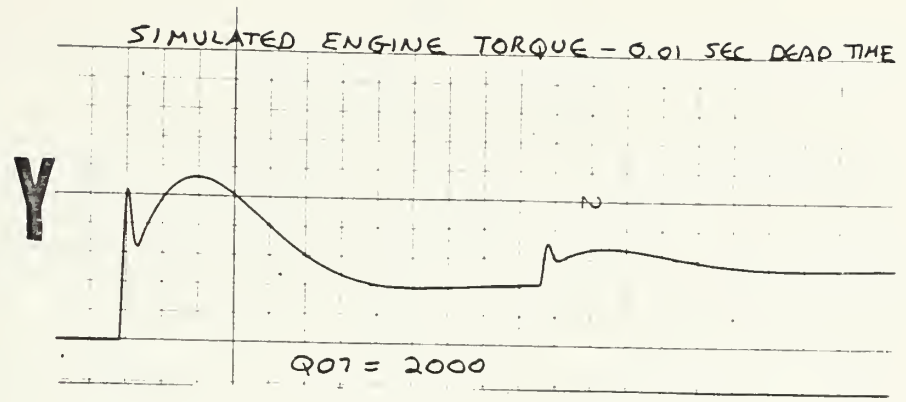

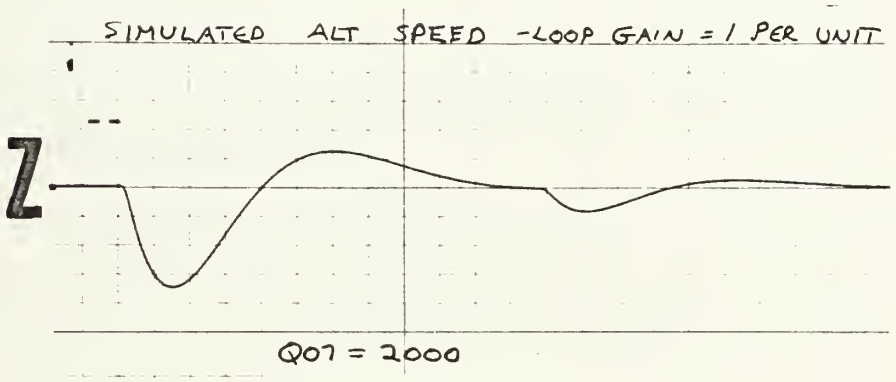

Figure 10.

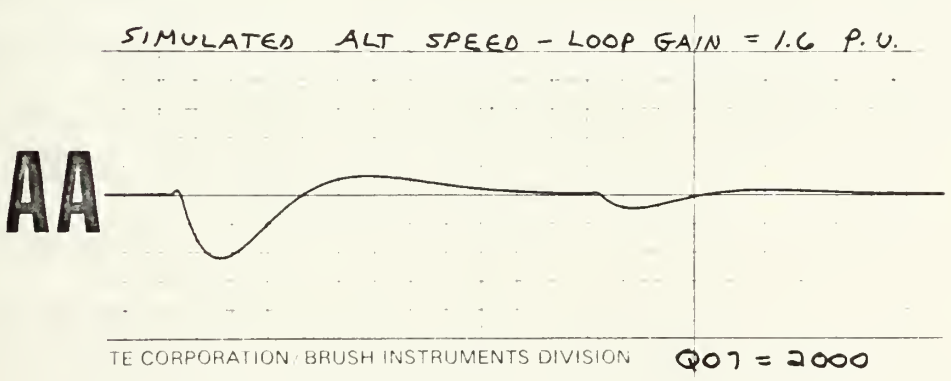

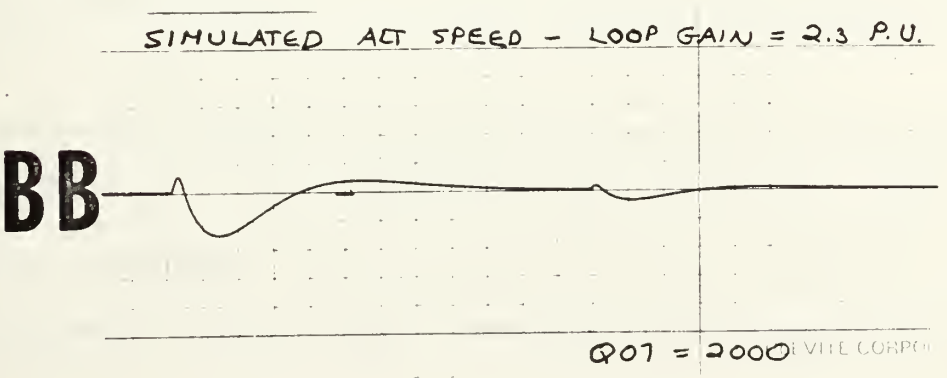

DISCUSSION OF RESULTS

ALTERNATOR SPEED A comparison of strips A and B shows that there is excellent qualitative correlation between the simulation and the prototype performance. In the simulation the speed transient which occurs when the induction motor switches to speed five occurs approximately one second too late. This is due to an error in setting P90 which controls the switching time for motor speed five and in no way affects the validity of the model. The three criteria listed below give an indication of the quantitative correlation for the first speed transient.

(1) Maximum deviation in speed--For the prototype the drop in frequency is eighteen chart divisions at a sensitivity of 20 mv/division. The frequency converter sensitivity is 2.5V/5Hz. The frequency deviation is 0.72 Hz which corresponds to a 0.24 rev/sec drop in alternator speed. In the simulation the speed drop was 1.5 rad/sec or 0.239 rev/sec.

(2) Ratio of speed drop to speed overshoot--Comparing the simulation and prototype gives the following approximate values:

Simulation - 3.34

Prototype - 3.60

(3) Time to return to original speed--For both simulation and prototype the speed first returned to synchronous speed in approximately 0.70 seconds.

The correlation noted above is admittedly a retrofit to the prototype data. However, it is clearly shown that the model used closely predicts the prototype performance. In the simulation the engine parameters set on the potentiometers were the values determined in the previous section.

The only settings which varied were the governor loop gain and the gain on the governor feedforward signal. These two settings are varied in the simulations to show their effects on engine performance.

The simulated output of the feedforward network is shown on strip Q. As expected this signal shows the derivative operation in the FFWD network. Strips M through P show the effect of increasing the FFWD gain. On strip P the speed shows an initial increase when the load is applied. This type of response is not possible for the system under study so that an upper limit must be imposed on Q07 which corresponds to the FFWD gain. However, the trend in engine performance as Q07 is increased is evident. The effect of the FFWD on engine torque is shown in strips K and L.

The effect of loop gain on performance is shown in strips Z, AA and BB. As gain is increased the speed deviations become smaller. In strips AA and BB it is evident that the FFWD gain is set too high since the speed shows a slight initial increase as load is applied. However, the influence of loop gain is still clear.

In deriving the turbine model, the engine dead time was assumed to be negligible or at least less than 0.01 seconds. The influence of dead time on response is shown in strips U through Y. The dead time is simulated using a first order lag approximation. In strip U the speed response for 0.1 seconds dead time is shown. The response is noticeably worse than that shown on strip N which is the response for the same potentiometer settings for all components and with no dead time. The reason for the deterioration in response is evident from comparing strips V and W. The dead time causes the torque to lag the fuel actuator angle as shown. Strips X and Y correspond to a dead time of 0.01 second. Comparison of the speed response

shown on strips X and N shows that there is no noticeable difference in response. As a result, any dead time less than 0.01 second can be neglected.

ALTERNATOR LOAD Strip C is the alternator KW load as measured by the governor load sensing section and as viewed through the 0.068 sec. LPF. Since the maximum alternator speed variation is on the order of one percent of base speed the load is roughly proportional to the alternator torque. The load signal was not calibrated to a known level of load so that this measurement may be used only for a qualitative comparison. Two ratios are used below to give an indication of the degree of correlation. The overshoot ratio compares the maximum torque for each transient to the steady torque level at the corresponding induction motor speed. The steady state ratio compares the steady torque at each induction motor speed to the steady torque at the maximum motor speed.

Table 3.

	OVERSHOOT RATIO		STEADY RATIO	
IM SPEED	SIM	PROTO	SIM	PROTO
1	2.80	2.00	.47	.55
2	1.29	1.24	.65	.70
3	1.16	1.14	.72	.78
4	1.25	1.19	.84	.87
5	1.61	1.37	1.00	1.00

The differences between simulated and observed values is due primarily to the difference between estimated and actual rotor resistance values.

A rough check can be made on the actual magnitude of the simulated

alternator torque. At speed five the induction motor torque is approximately 1400 lb-ft at 1150 RPM. Since the alternator speed is approximately 1200 RPM and the power levels of the alternator and induction motor are approximately equal, the alternator torque will be approximately 1400 lb-ft. The scaled value for the simulated alternator torque is 1350 lb-ft.

INDUCTION MOTOR The correlation of the induction motor performance and the simulation is given in Table 4 below. The values for the motor torque and current were taken from the motor performance curve, Figure 11. Also shown on this curve are the simulated values for torque and current.

Table 4.

Speed Position	RPM Obs.	RPM Sim.	Torque (Performance Curve)	i_{RMS}	Torque Simulated	i_{RMS}
1	834	840	800	-	700	200
2	966	960	1000	310	915	250
3	1032	1015	1100	340	1030	275
4	1104	1080	1270	380	1190	300
5	1180	1150	1450	425	1380	350

As with the engine simulation the results can vary widely depending on the values used for the motor and propeller parameters. The original estimates for the motor inertia and the rotor resistances were changed slightly in order to provide a better fit between the model and the observed performance. The differences between the original parameter estimates and the values used in the simulation are summarized in Table 5.

Table 5.

Parameter	Estimated Value	Potentiometer	Setting From Scaled Eqn.	Setting Used
X_{sm}	.71 ohms	P10	$8460(10^3)$	$8277(10^3)$
R_a	.0117	P03	0220	0597
$R_{a(1)}$	.240	P00	4450	6000
$R_{a(2)}$	.088	P32	1660	2000
$R_{a(3)}$	.072	P65	1360	2000
$R_{a(4)}$	.063	P95	1190	2000
I_m+I_p	21.6	P35	1475(10)	2000(10)
K_p	1.08×10^{-3}	P67	3880	3880

All parameters agree with the estimated values except for the rotor resistances and the motor inertia. The difference in inertia is not large and is within the accuracy of the original estimate. The potentiometer settings corresponding to values of R_a were considerably higher than the original estimates. These higher settings result from the fact that a single-phase model is being used to represent a three-phase machine.

For the three phase delta connected rotor the resistance is given as 0.0117 ohms. This resistance was probably measured across the slip rings and would correspond to the following diagram.

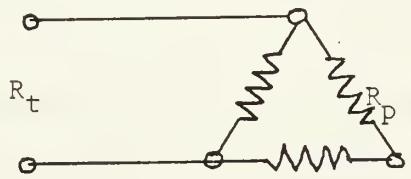

As a result the single phase equivalent resistance (R_p) is 1.5 R_t. This requires that the settings for the potentiometers representing the rotor

resistances in the table above be increased by a factor of 1.5. The values given in the manufacturer's drawings for the switched resistors are assumed to be nominal values. For this simulation the same value (.70 ohms) was used for resistors two, three and four with resistor one assumed to be three times as large. These values are very close to the specified nominal values and give excellent qualitative correlation for the transient currents.

With R_t for the rotor given as 0.0117 ohms and corrected to a single phase equivalent the required setting on P03 is 0032 whereas a setting of 0597 was used in the simulation. A value of 0032 was used but the current surge when switching to speed five was larger than observed on the prototype. As would be expected, the current transients at the other switching points were not noticeably affected by this change in the residual rotor resistance. The difference between the required rotor resistance potentiometer setting and the value actually used is due to the fact that at this point the divider A03 which is generating the motor back emf is poorly scaled for Analog computation and accuracy is limited.

When P65 is switched out of the motor resistance network the operation at A03 is as follows:

$$v = \frac{R_a \, I}{N_s - N}$$

At the switching point $(N_s - N)$ is approximately 0.12 per unit and approaches 0.05 P.U. in the limit. With (I) properly scaled to avoid saturation at all other transients the magnitude of (I) at switching is approximately 0.3 P.U. With R_a set at 0300 the component A03 is dividing a small signal by a small signal. As a result accuracy at this point is limited. A03 can be rescaled to give higher accuracy when N approaches N_s but this will cause saturation

when the motor is first started. The divider must be constrained to operate at all times with the numerator smaller in magnitude than the denominator.

Even with the reduced accuracy, when the motor speed approaches synchronous speed, there is still good correlation between the simulation and the prototype performance throughout the entire operating range. Strips E through H show the correlation of speed and current. The data tabulated above is plotted on the motor performance curve, Figure 11, and shows the quantitative correlation for torque and current. The simulated current shows the same trend as the performance curve data but is lower at all points. This is due in part to the error in measuring the magnitudes of the current from the strip recording.

FIGURE 11

INDUCTION MOTOR PERFORMANCE CURVES WITH SIMULATION RESULTS

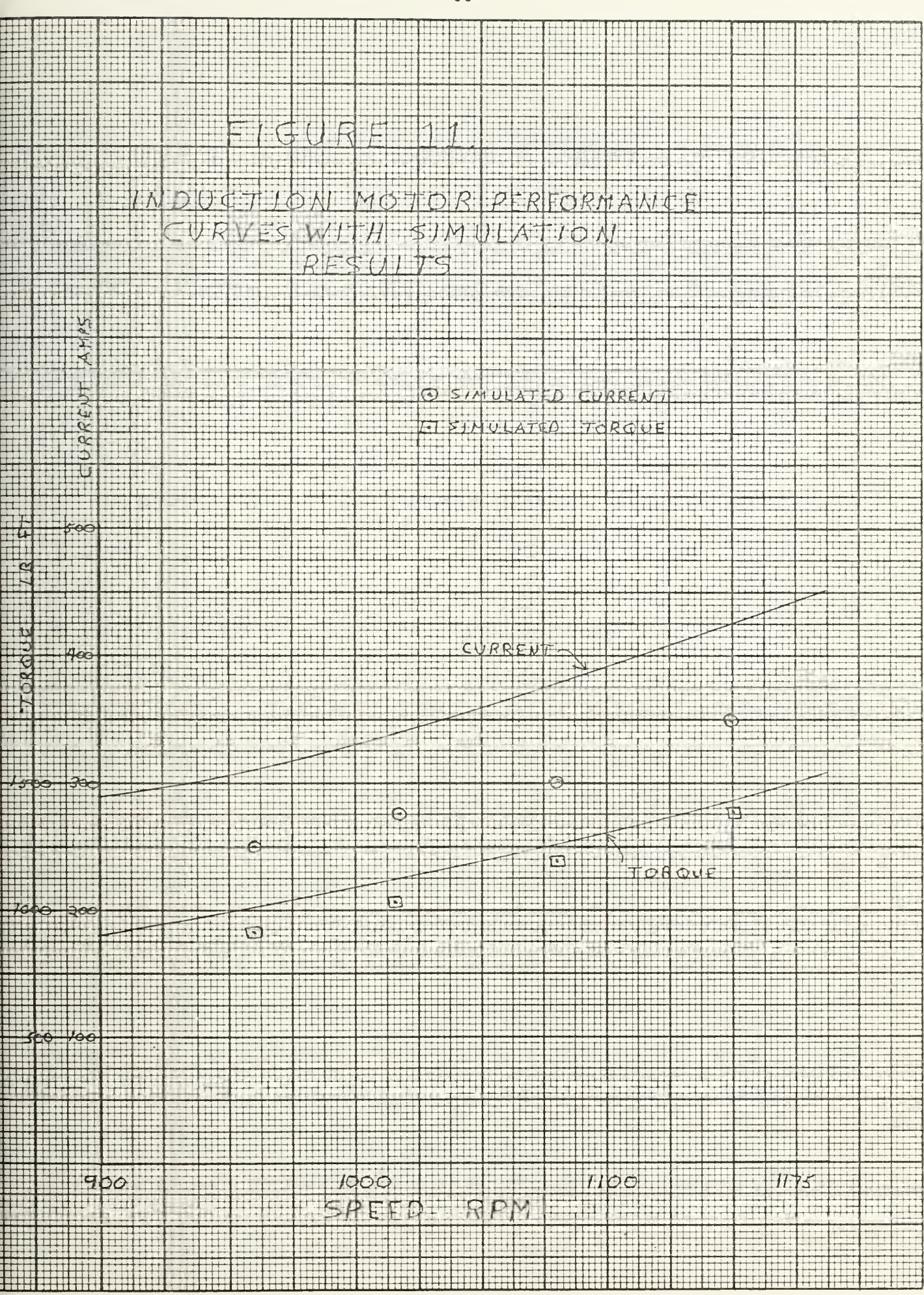

7. CONCLUSIONS AND RECOMMENDATIONS

The correlation between the simulation and prototype for all observed variables proves the validity of the models used in the simulation. The natural tendency is to expect that highly complex models will be required for each component. However, reasonable accuracy in quantitative predictions and highly valuable qualitative information about system performance have been obtained using simple "off the shelf" models. The simulation can be helpful in design or as a training aid.

As indicated earlier, the simulation gives the designer an indication of trends in system performance as the various parameters are adjusted. For a given motor the parameters X_{sm} and R_a are fixed. The switched resistors and switching times are the two most important parameters which can also be easily adjusted. The simulation shows how the performance can be varied over a wide range by adjusting these parameters. Although the designer has little control over the inertia of the motor and propeller, the inertia effects are clearly shown. Finally, the effects of propeller pitch as characterized by the propeller torque coefficient can be investigated.

The simulation provides an excellent study of the governing system and engine performance. The most important governor adjustments are controllable by potentiometer settings so that changes in the governor coefficients can be investigated. The effects on engine torque and speed response are clearly shown. In addition to providing useful design information, the simulation can demonstrate to operating personnel the effects on system performance due to changes in the governor settings.

The transfer function approach to modeling the prime mover yielded a

simulation which can easily be adapted to any other type of prime mover by substituting the proper transfer function (on a diode function generator if necessary) in the place of the gas turbine model. The model used in this simulation is readily adaptable for use with diesel engines with the most significant change being in the assumed engine dead time.

The two most important dynamic effects which were not included in the simulation because of the limitation on computing hardware were the voltage regulation and fuel control valve effects. With additional hardward these effects can easily be included. However, as the results indicate, neglect of these effects did not seriously affect the accuracy of the simulation.

Neglecting the stabilizer section of the governor control box and dynamics of the fuel control valve did not seriously affect the results for two reasons. The input disturbances to the gas turbine were below the frequency level where the stabilizer section influences performance. Although the load transient was close to a step change the second order filter on load inputs to the gas turbine limits change to approximately 12 Hz. Also, in scaling the simulation the developed engine torque was limited to 3000 lb-ft. This provides a form of acceleration limiting.

Neglect of the voltage regulation effects can influence the results in two ways. First, in the simulation the induction motor is supplied with a constant voltage whereas in the prototype the voltage varies as shown in Strip S. The error caused by this assumption is not serious. The second effect of neglecting the voltage regulation is on alternator torque. With field current assumed constant, the gyrator modulus on the alternator is constant so that the torque is directly proportional to the line current.

The field current does increase slightly during the transients so that the prototype alternator torque is higher than shown on strip J. However, the correlation between the simulation and prototype performance shows that considering field current constant does not cause a serious error.

The use of a single-phase model for the three-phase machine introduces no serious errors. The inertia of the induction motor is large enough so that the double frequency torque pulsations in the motor are not noticed. At the alternator end, the second order filter provided adequate filtering of the pulsations and adequate frequency response in order to pass the transient loads. Even with unlimited Analog hardware it would not be necessary to use a three-phase model as the single-phase model is more than adequate.

RECOMMENDATIONS

The observed system performance indicates that the original system design is more than adequate in order to meet its performance specifications. Therefore, use of this simulation in an attempt to improve the overall design is not practical. The only change to the original system which could be made at small cost is in the starting resistors. The speed range of the motor with the installed resistors is from approximately 65 to 95 percent of synchronous speed. This range could be extended by changing the resistors. The required resistors and dynamic performance can be determined by the simulation. However, it is not practical to lower the speed significantly because then the motor will be operating at a very low efficiency.

One area where additional work may be done is in utilizing the hybrid capabilities of the computer facility. Although the simulation has been done with only the Analog computer, the hybrid facility can be utilized to increase the effectiveness of the simulation. One very interesting study would be to perform an optimization study of the system. Even though prototype system performance is adequate, such a study would give a student the opportunity to learn the basics of hybrid computing and to study in the area of optimal control.

The most important dynamic elements which were neglected were the fuel control valve and the voltage regulator. The governor control box stabilizer section was also neglected. Since the simulation required approximately 90 percent of the Analog hardware, it would be difficult to include reliable models of these components. A more detailed study of the generator set alone can be performed by replacing the induction motor load by a step load change. It will then be possible to include the effects of the fuel control valve, voltage regulator and stabilizing section.

The generator set frequency regulation is extremely important for proper operation of the shipboard electronic equipment. As a result, the speed deviations of the gas turbine must be kept to a minimum when the generator is supplying power to the electronic equipment. A simulation of the generator set in response to step load changes can be used to design the governing system and to determine the governor settings required for best performance.

The most direct benefit of the simulation would be to use it to demonstrate to operating personnel how the system performance can be altered by adjusting the governor settings. The desire to "leave well enough alone"

together with a lack of complete understanding of how a system operates will usually prevent operators from adjusting the governor to get better performance. The simulation can be used to instruct operators in how the various governor settings effect performance. With a better understanding of how the system behaves, it will be easier to adjust the governor settings for near optimum performance.

REFERENCES

(1) Paynter, H.M., "Hydraulics by Analog--An Electronic Model of a Pumpint Plant," J. Boston Soc. of Civil Engineers, July 1959, pp. 197-219.

(2) Woodward Governor Company, "EG-A Control Box," Woodward Governor Company, Rockford, Illinois.

(3) EAI Inc., Handbook of Analog Computation, published by Electronic Associates, Inc., 1967.

(4) EAI, Inc., 680 Reference Handbook, published by Electronic Associates, Inc., 1967.

(5) Karnopp, D. and Rosenberg, R., Analysis and Simulation of Multiport Systems, published by the M.I.T. Press, 1968.

(6) Ferre, G. and Lenkaitis, D., "Gas Turbine Engine Analog Simulation for Acceleration Sensing Fuel Control Studies," from Gas Turbine Fuel Controls Analysis and Design, published by Society of Automotive Engineers, 1965.

(7) Del Toro, V., Principles of Electrical Engineering, published by Prentice-Hall, Inc., 1965.

(8) Paynter, H., and Karnopp, D., "Design and Control of Multiport Engineering Systems," Proceedings of IFAC Tokyo Symposium on Systems Engineering for Control System Design, 1965.

(9) Fitzgerald, A., and Kingsley, C., Electric Machinery, published by McGraw-Hill Book Company, 1961.

(10) "First Interim Technical Report, Computer Simulation of The Power Conversion System for Nike-X Power Plants," 1 March to 15 July 1965, Arthur D. Little, Inc., Cambridge, Massachusetts.